Integrin β4 promotes DNA damage drug resistance in triple-negative breast cancer via TNFAIP2/IQGAP1/Rac1

Huan Fang[1, 2#], Wenlong Ren[1,3#], Qiuxia Cui[4, 5, 1#], Huichun Liang[1#], Chuanyu Yang[1], Wenjing Liu[1], Xinye Wang[1], Xue Liu[6], Yujie Shi[7*], Jing Feng[8, 6*], Ceshi Chen[9,10,1*]

1. Key Laboratory of Animal Models and Human Disease Mechanisms, Kunming Institute of Zoology, Chinese Academy of Sciences. Kunming, Yunnan, China.

2. Kunming College of Life Sciences, University of Chinese Academy Sciences, Kunming, Yunnan, China.

3. School of Life Science, University of Science & Technology of China. Hefei, Anhui, China.

4. Affiliated Hospital of Guangdong Medical University. Zhanjiang, Guangdong, China.

5. Department of Breast Surgical Oncology, National Cancer Center/National Clinical Research Center for Cancer/Cancer Hospital & Shenzhen Hospital, Chinese Academy of Medical Sciences and Peking Union Medical College, Shenzhen, Guangdong, China.

6. Shanghai University of Medicine & Health Sciences, Affiliated Sixth People's Hospital South Campus, Shanghai, China.

7. Department of Pathology, Henan Provincial People's Hospital, Zhengzhou University, Zhengzhou, Henan, 450003, China.

8. The Second Affiliated Hospital of the Chinese University of Hong Kong (Shenzhen), Shenzhen, 518172, China.

9. Academy of Biomedical Engineering, Kunming Medical University, Kunming 650500, China.

26 10. The Third Affiliated Hospital, Kunming Medical University, Kunming 650118,
27 China.

28

29 Short Title: ITGB4 promotes drug resistance in TNBC through TNFAIP2

30

31 [#] These authors contribute equally

32

33 * Corresponding authors: Ceshi Chen, E-mail: chenc@kmmu.edu.cn, Jing Feng,
34 E-mail: fengjing71921@163.com, or Yujie Shi, E-mail: shiyujie523@126.com

35

Summary

Anti-tumor drug resistance is a challenge for triple-negative breast cancer treatment. Our previous work demonstrated that TNFAIP2 activates Rac1 to promote triple-negative breast cancer cell proliferation and migration. However, the mechanism by which TNFAIP2 activates Rac1 is unknown. In this study, we found that TNFAIP2 interacts with IQGAP1 and Integrin β4. Integrin β4 activates Rac1 through TNFAIP2 and IQGAP1 and confers DNA damage drug resistance in triple-negative breast cancer. These results indicate that the Integrin β4/TNFAIP2/IQGAP1/Rac1 axis provides potential therapeutic targets to overcome DNA damage drug resistance in triple-negative breast cancer.

Keywords

ITGB4, TNFAIP2, IQGAP1, Rac1, drug resistance, DNA damage repair, triple-negative breast cancer

Introduction

Breast cancer is the most common malignant tumor in women, and the morbidity and mortality rates of female malignant tumors are ranked first in the world[1]. Although the diagnosis and treatment of breast cancer has entered the era of molecular typing,35% of breast cancers still experience recurrence, metastasis and treatment failure[2]. According to the expression of estrogen receptor (ERα), progesterone receptor (PR) and human epidermal growth factor receptor (HER2), breast cancer is divided into ER/PR-positive, HER2-positive and triple-negative breast cancer (TNBC)[3].For ER/PR-positive and HER2-positive breast cancer, endocrine therapies such as tamoxifen and anti-HER2 targeted therapy such as trastuzumab have achieved good efficacy. Targeted drugs for TNBC patients with BRCA1/2 mutations include two PARP inhibitors, olaparib and talazoparib. These targeted drugs cannot fully meet the clinical needs of patients with various TNBC subtypes[4]. Currently, DNA damage chemotherapy drugs, including epirubicin and cisplatin, are widely used for TNBC treatment.

TNBC often recurs and metastasizes due to the development of chemoresistance, although it is initially responsive to chemotherapeutic drugs[5]. Chemoresistance severely impacts the clinical outcomes of patients. Tumor cells become resistant to chemotherapeutic agents through several mechanisms, such as improving DNA damage repair, changing the

intracellular accumulation of drugs, or increasing anti-apoptotic mechanisms[6]. Therefore, characterization of the underlying molecular mechanisms by which resistance occurs will provide opportunities to develop precise therapies to enhance the efficacy of standard chemotherapy regimens [7,8].

TNFAIP2 is abnormally highly expressed in a variety of tumor cells, including TNBC[9], nasopharyngeal carcinoma [10], malignant glioma[11], uroepithelial carcinoma[12]and esophageal squamous cell carcinoma[13], and is associated with poor prognosis. Our previous work [9,14]showed that TNFAIP2, as a KLF5 downstream target protein, can interact with Rac1[15], a member of the Rho small GTP enzyme family, and activate Rac1 to alter the cytoskeleton, thereby inducing filopodia and lamellipodia formation and promoting the adhesion, migration and invasion of TNBC cells. After activation, Rac1 can activate AKT, PAKs, NADPH oxidase and other related signaling pathways to promote cell survival, proliferation, adhesion, migration and invasion[16]. Activation of Rac1 can reduce the therapeutic response to trastuzumab in breast cancer and increase the resistance of TNBC cells to paclitaxel[17], but the specific mechanism of action is not completely clear.

Rac1 has been shown to play an important role in DNA damage repair. Activated Rac1 can promote the phosphorylation of the DNA damage response-related molecules ATM/ATR, CHK1/2 and H2AX by activating the

activity of protein kinases such as ERK1/2, JNK and p38 [18,19], thus improving the DNA damage repair ability and inhibiting tumor cell apoptosis[20-22]. Rac1 also promotes aldolase release and activation by changing the cytoskeleton and activates the ERK pathway to increase thepentose phosphate pathway to promote nucleic acid synthesis, providing more raw materials for DNA damage repair[23,24]. At the same time, the interaction of Rac1 and PI3K promoted AKT phosphorylation and glucose uptake[25,26]. Therefore, Rac1 is well established to promote the chemoresistance of breast cancer by promoting DNA damage repair.

Integrin β4 (ITGB4) is a major component of hemidesmosomes and a receptor molecule of laminin. Studies have shown that laminin-5 interacts with ITGB4 to activate Rac1 activity and promote cell migration[27] and polarization[28] by altering the cytoskeleton. Since ITGB4-positive cancer stem cell (CSC)-enriched mesenchymal cells were found to reside in an intermediate epithelial/mesenchymal phenotypic state, ITGB4 can be used to enable stratification of mesenchymal-like TNBC cells[29]. In addition, the expression of ITGB4 on $ALDH^{high}$ breast cancer and head and neck cancer cells was significantly greater than that on $ALDH^{low}$ cells, proving the effects that ITGB4 targets on both bulk and CSC populations[30]. Furthermore, ITGB4-overexpressing TNBC cells provided cancer-associated fibroblasts (CAFs) with ITGB4 proteins via exosomes, and ITGB4-overexpressing

117 CAF-conditioned medium promoted the proliferation,
118 epithelial-to-mesenchymal transition, and invasion of breast cancer cells[31].
119 ITGB4 also promotes breast cancer cell resistance to tamoxifen-induced
120 apoptosis by activating the PI3K/AKT signaling pathway and promotes breast
121 cancer cell resistance to anoikis by activating Rac1[32]. However, how ITGB4
122 activates Rac1 is not completely clear.
123
124 Rac1 activity is regulated by guanylate exchange factors (GEFs), GTPase
125 activation proteins (GAPs), and guanine separation inhibitors (GDIs)[33]. GAPs
126 typically provide the necessary catalytic groups for GTP hydrolysis, but not all
127 GAPs function as hydrolases. IQGAP1 lacks an arginine in the GTPase
128 binding domain and cannot exert the hydrolysis effect of GAPs[34]. IQGAP1 can
129 increase the activity of Rac1 and CDC42[35,36].
130
131 In this study, we demonstrated that TNFAIP2 interacts with IQGAP1 and
132 ITGB4. ITGB4 promotes TNBC drug resistance via the
133 TNFAIP2/IQGAP1/Rac1 axis by promoting DNA damage repair. Our results
134 suggest that ITGB4 and TNFAIP2 might serve as promising therapeutic targets
135 for TNBC.
136

137 **Results**

138 **TNFAIP2 promotes TNBC DNA damage drug resistance**

139 To explore the functional significance of TNFAIP2 in TNBC drug resistance, we
140 constructed stable TNFAIP2 overexpression and TNFAIP2 knockdown
141 HCC1806 and HCC1937 cells. As shown in Figure 1A-E, overexpression of
142 TNFAIP2 significantly increased cell viability when treated with EPI and BMN.
143 Additionally, knockdown of TNFAIP2 significantly decreased cell viability when
144 treated with EPI and BMN (Fig. 1F-J). We then examined the effects of
145 TNFAIP2 on DNA damage repair and found that TNFAIP2 promotes DNA
146 damage repair in response to EPI and BMN. TNFAIP2 overexpression
147 decreased the protein expression levels of γH2AX, a marker of DNA damage,
148 and cleaved-PARP, a marker of apoptosis (Fig. 1K). Additionally, knockdown of
149 TNFAIP2 significantly increased γH2AX and cleaved-PARP protein expression
150 levels in response to EPI and BMN in both cell lines (Fig. 1L).

151

152 The function of TNFAIP2 was further validated by using two other DNA
153 damage drugs, DDP and AZD (Fig. S1A-L). These results suggested that
154 TNFAIP2 enhances TNBC cell drug resistance by promoting DNA damage
155 repair.

156

157 **TNFAIP2 confers TNBC drug resistance *in vivo***

158 To test whether TNFAIP2 also decreases the sensitivity of TNBC cells to EPI

159 and BMN *in vivo*, we performed animal experiments in nude mice. HCC1806
160 cells with stable TNFAIP2 knockdown were orthotopically inoculated into the
161 fat pad of 7-week-old female mice (n=8 or 12/group). When the tumor mass
162 reached approximately 50 mm^3, each group was divided into two subgroups to
163 receive either EPI (2.5 mg/kg, twice a week) or vehicle control for 23 days and
164 either BMN (1 mg/kg, twice a week) or vehicle control for 29 days. We
165 observed that depletion of TNFAIP2 suppressed breast cancer cell growth *in*
166 *vivo*. This is consistent with our previous report[9]. More importantly, TNFAIP2
167 depletion further decreased tumor volume when mice were treated with EPI
168 and BMN (Fig. 2A-F). Meanwhile, BMN treatment had no effect on the body
169 weight of mice (Fig. S2F). Consistently, EPI and DDP generated similar results
170 but decreased mouse body weight due to their high toxicity (Fig.S2D-E). These
171 results suggest that inhibition of TNFAIP2 expression can overcome HCC1806
172 breast cancer cell drug resistance in animals.
173

174 **TNFAIP2 promotes TNBC drug resistance and DNA damage repair via**
175 **Rac1**

176 Since chemotherapeutic agents and PRAP inhibitors induce DNA damage
177 directly or indirectly, DNA damage repair ability profoundly affects the
178 sensitivity of cancer cells to these therapies[37,38]. Since TNFAIP2 can activate
179 Rac1, a well-known drug resistance protein, we investigated whether TNFAIP2
180 induces chemotherapeutic resistance through Rac1. We found that Rac1

181 knockdown rescued the effects of TNFAIP2 overexpression-induced drug
182 resistance to EPI and BMN in HCC1806 and HCC1937 cells (Fig. 3A-F). We
183 also found that γH2AX and cleaved-PARP protein levels were up-regulated
184 again in Rac1 knockdown and TNFAIP2-overexpressing HCC1806 and
185 HCC1937 cells in response to EPI and BMN (Fig. 3G-J). We obtained similar
186 results by using DDP and AZD treatment (Fig. 3SA-J). Collectively, these
187 results suggest that TNFAIP2 promotes DNA damage repair and drug
188 resistance via Rac1.
189

190 **IQGAP1 mediates Rac1 activation by TNFAIP2 and promotes TNBC drug**
191 **resistance**

192 To characterize the mechanism by which TNFAIP2 activates Rac1, we
193 performed an IP-MS experiment. We found that TNFAIP2 interacts with
194 IQGAP1 (Fig. 4A). To validate whether TNFAIP2 interacts with IQGAP1, we
195 constructed HCC1806 cells with stable Flag-TNFAIP2 overexpression and
196 collected Flag-tagged TNFAIP2 cell lysates for immunoprecipitation assays
197 using Flag-M2 beads (Fig. S4A). We performed immunoprecipitation using
198 ananti-IQGAP1 antibody and found that endogenous IQGAP1 protein
199 interacted with endogenous TNFAIP2 protein inHCC1806 cells (Fig. 4B). Next,
200 we mapped the regions of TNFAIP2 and IQGAP1 proteins responsible for the
201 interaction by generating a series of Flag-TNFAIP2 deletion mutants and
202 transfected them into HEK293T cells together with full-length IQGAP1. Then,

203 we performed immunoprecipitation assays using Flag-M2 beads (Figure S4B),
204 and the N-terminus (1-79 aa) of the TNFAIP2 protein interacted with IQGAP1.
205 To explore the function of IQGAP1 in TNBC drug resistance, we knocked down
206 IQGAP1 in HCC1806 and HCC1937 cells. As shown in Figure 4C-G,
207 knockdown of IQGAP1 significantly decreased cell viability in the presence of
208 EPI and BMN in both cell lines. We also examined the effects of IQGAP1 on
209 DNA damage repair and found that IQGAP1 promotes DNA damage repair.
210 IQGAP1 knockdown increased γH2AX and cleaved-PARP protein expression
211 levels when HCC1806 and HCC1937 cells were treated with EPI and BMN
212 (Fig. 4H). Next, we found that IQGAP1 knockdown abrogated the effects of
213 TNFAIP2 overexpression on resistance to EPI and BMN (Fig. 4I-K, Fig.
214 S4C-E). We also found that γH2AX and cleaved-PARP protein levels were
215 up-regulated in IQGAP1 knockdown and TNFAIP2-overexpressing HCC1806
216 and HCC1937 cells (Fig. 4L). In addition, we found that the TNFAIP2
217 overexpression-induced increase in Rac1 activity was abolished by IQGAP1
218 knockdown (Fig. 4M).
219

220 **ITGB4 interacts with TNFAIP2 and promotes TNBC drug resistance and**
221 **DNA damage repair**

222 In addition to IQGAP1, TNFAIP2 may interact with ITGB4 (Fig. 4A). To validate
223 whether TNFAIP2 interacts with ITGB4, we immunoprecipitated exogenous
224 Flag-tagged TNFAIP2 proteins from HCC1806 cells by using Flag-M2 beads

225 and detected endogenous ITGB4 proteins(Fig. 5A).To further confirm the
226 protein–protein interaction between endogenousTNFAIP2 and ITGB4proteins,
227 we collected HCC1806 cell lysates and performed immunoprecipitation using
228 an anti-TNFAIP2/ITGB4 antibody and found that endogenous TNFAIP2/ITGB4
229 protein interacted with endogenous ITGB4/TNFAIP2 protein (Fig. 5B-C).We
230 further mapped the regions of TNFAIP2 and ITGB4 proteins responsible for the
231 interaction(Fig. S5I) by generating a series of Flag-TNFAIP2/GST-fused
232 TNFAIP2 deletion mutants and transfected them into HEK293T cells together
233 with full-length GST-fused ITGB4/ITGB4. Then, we performed
234 immunoprecipitation assays using Flag-M2 beads and glutathione beads. As
235 shown in Figure S5J-K, the N-terminus (218-287 aa) of the TNFAIP2
236 (TNFAIP2-S-N1-3) protein interacted with ITGB4. To map the domains of
237 ITGB4 that interact with TNFAIP2, we transfected Flag-tagged full-length
238 TNFAIP2 into HEK293T cells with full-length or truncated ITGB4. We found
239 that the C-terminus (710-740 aa) of the ITGB4 protein interacted with TNFAIP2
240 (Fig. S5L-M). Taken together, these results suggest that TNFAIP2 interacts
241 with ITGB4 and that their interaction is mediated through the N-terminus of
242 TNFAIP2 and the C-terminus of ITGB4.
243 To explore the function of ITGB4 in TNBC drug resistance, we knocked down
244 ITGB4 in HCC1806 and HCC1937cells. As shown in Figure 5D-I, knockdown
245 of ITGB4 significantly decreased cell viability in the presence of EPI and BMN
246 in both cell lines. Knockdown of ITGB4 also suppressed HCC1806 xenograft

247 growth *in vivo*. More importantly, ITGB4 knockdown further decreased tumor
248 volume when mice were treated with EPI and BMN (Figure. 5J-N). Meanwhile,
249 BMN treatment had no effect on the body weight of mice, but EPI treatment
250 decreased mouse body weight due to its toxicity (Fig. S5H). We then
251 examined the effects of ITGB4 on DNA damage repair and found that ITGB4
252 promotes DNA damage repair in response to EPI and BMN. ITGB4 knockdown
253 increased γH2AX and cleaved-PARP protein expression levels when
254 HCC1806 and HCC1937 cells were treated with EPI and BMN (Fig. 5O).
255 Furthermore, the function of ITGB4 was validated by using two other drugs,
256 DDP and AZD (Fig. S5A-G). These results suggested that ITGB4 increases
257 TNBC drug resistance and promotes DNA damage repair.
258

259 **ITGB4 activates Rac1 through TNFAIP2 and IQGAP1**

260 It is well known that ITGB4 can activate Rac1[27] and that TNFAIP2 interacts
261 with Rac1 and activates it[9]. To test whether ITGB4 activates Rac1 through
262 TNFAIP2, we measured the levels of GTP-bound Rac1 in
263 ITGB4-overexpressing and ITGB4-knockdown cells. Overexpression of ITGB4
264 significantly increased the levels of GTP-bound Rac1 in bothHCC1806 and
265 HCC1937 cells (Fig. 6A). In agreement with this observation, knockdown of
266 ITGB4 significantly decreased the levels of GTP-bound Rac1 in both cell lines
267 (Fig. 6B). Next, we knocked down TNFAIP2 in ITGB4-overexpressing
268 HCC1806 and HCC1937 cells and found that ITGB4-increased Rac1 activity

269 was blocked by TNFAIP2 knockdown (Fig. 6C-D). Collectively, these results
270 demonstrate that ITGB4 activates Rac1 through TNFAIP2.
271
272 It has been reported that Rac1 activity is promoted by IQGAP1[34] and that
273 TNFAIP2 activates Rac1 through IQGAP1 (Fig. 4P). We wondered whether
274 ITGB4 activates Rac1 through IQGAP1; therefore, we knocked down IQGAP1
275 in HCC1806 and HCC1937 cells with stable overexpression of ITGB4 and
276 found that the ITGB4-induced increase in Rac1 activity was abolished by
277 IQGAP1 knockdown (Fig. 6E-F). These results suggest thatITGB4 activates
278 Rac1 through TNFAIP2 and IQGAP1.
279
280 **ITGB4 promotes TNBC drug resistance via TNFAIP2/IQGAP1/Rac1**
281 Since ITGB4, TNFAIP2, and IQGAP1 promote drug resistance by promoting
282 DNA damage repair in TNBC, we wondered whether ITGB4 promoted drug
283 resistance through the TNFAIP2/IQGAP1/Rac1 axis. We knocked down
284 TNFAIP2, IQGAP1, and Rac1in ITGB4-overexpressing cells and found that
285 blocking the TNFAIP2/IQGAP1/Rac1 axis increased the sensitivity of
286 ITGB4-overexpressing HCC1806 (Fig. 7A-I) and HCC1937 cells to EPI and
287 BMN (Fig. S6O-W).We also found that γH2AX and cleaved-PARP levels were
288 upregulated in TNFAIP2/IQGAP1/Rac1 knockdown HCC1806 and HCC1937
289 cells stably expressing ITGB4 in the presence of EPI and BMN (Fig. 7J-L, Fig.
290 S6X-Z). DDP and AZD treatment generated similar results (Fig. S6A-N).

291 Together, these results suggest that ITGB4 promotes DNA damage repair and
292 drug resistance via the TNFAIP2/IQGAP1/Rac1 axis.
293
294 **TNFAIP2 expression levels positively correlated with ITGB4 in TNBC**
295 **tissues**
296 To test whether ITGB4 and TNFAIP2 are coexpressed in TNBC, we collected
297 135 TNBC specimens for IHC (the IQGAP1 antibody did not work for IHC).
298 Clinical pathological parameters, including patient age, tumor size, lymph node
299 status at the time of diagnosis, and follow-up status, including adjuvant
300 treatment and tumor recurrence, were retrospectively obtained from the
301 Department of Pathology, Henan Provincial People's Hospital, Zhengzhou
302 University, China. We performed IHC analyses on two breast cancer tissue
303 chips containing a total of 135 patients with TNBC (Fig. 8A-D).TNFAIP2 and
304 ITGB4 protein expression levels were significantly positively correlated(Table
305 1).
306

307 **Discussion**

308 Chemotherapies, including EPI and DDP, are the main choice for TNBC
309 patients. Unfortunately, TNBC frequently develops resistance to
310 chemotherapy[39]. Currently, PARP inhibitors are effective for TNBC with
311 BRCA1/2 mutation or homologous recombination deficiency (HRD)[40-42]. PARP
312 inhibitors can cause DNA damage repair defects and have synergistic lethal
313 effects with HRD. Meanwhile, chemotherapy and PARP inhibitor resistance is
314 also a major problem in the clinic.

315 In this study, we first found that TNFAIP2 promotes TNBC drug resistance and
316 DNA damage repair through Rac1. Next, we found that TNFAIP2 interacts with
317 IQGAP1 and ITGB4. We verified that ITGB4 promotes TNBC drug resistance
318 and DNA damage repair through the TNFAIP2/IQGAP1/Rac1 axis.
319 Interestingly, we discovered for the first time that ITGB4 and TNFAIP2 promote
320 Rac1 activity through IQGAP1. Our study reveals that ITGB4 promotes TNBC
321 resistance through TNFAIP2-, IQGAP1-, and Rac1-mediated DNA damage
322 repair (Figure 7). This study provides new targets for reversing TNBC
323 resistance.

324 ITGB4 is well known to promote breast cancer stemness and can be activated
325 by laminin 5[43]. In addition, ITGB4 is generally in partner with ITGA6, which is
326 another marker of breast cancer stem cells[44] and drug resistance[43]. Therefore,
327 whether ITGA6 has similar functions needs further study. It was reported that
328 ITGB4 activates Rac1[45], but the mechanism is unclear. For the first time, we

329 revealed that ITGB4 activates Rac1 through TNFAIP2 and IQGAP1. More
330 importantly, ITGB4 promotes drug resistance through the
331 TNFAIP2/IQGAP1/Rac1 axis.
332 TNFAIP2 plays important roles in different cellular and physiological processes,
333 including cell proliferation, adhesion, migration, membrane TNT formation,
334 angiogenesis, inflammation and tumorigenesis[14]. We previously found that
335 TNFAIP2 was regulated by KLF5 and interacted with the small GTPases Rac1
336 and Cdc42, thereby regulating the actin cytoskeleton and cell morphology in
337 breast cancer cells[9]. However, the detailed mechanism is not clearly
338 understood. In this study, we found that IQGAP1 mediates this
339 process.IQGAP1 is a crucial regulator of cancer development by scaffolding
340 and facilitating different oncogenic pathways, especially Rac1/Cdc42, thus
341 affecting proliferation, adhesion, migration, invasion, and metastasis[46]. In
342 addition, IQGAP1 is increased during the differentiation of ovarian cancer stem
343 cells and promotes aggressive behaviors[47]. In our study, we found that
344 TNFAIP2 interacts with IQGAP1 and thus activates Rac1 to induce
345 chemotherapy and PARP inhibitor drug resistance.
346 Furthermore, TNFAIP2 was reported to induce epithelial-to-mesenchymal
347 transition and confer platinum resistance in urothelial cancer cells[12], and in
348 embryonic stem cell (ESC) differentiation, TNFAIP2 was found to be important
349 in controlling lipid metabolism, which supports the ESC differentiation process
350 and planarian organ maintenance[48]. Another study found that TNFAIP2

351 overexpression enhanced TNT-mediated autophagosome and lysosome
352 exchange, preventing advanced glycation end product (AGE)-induced
353 autophagy and lysosome dysfunction and apoptosis[49]. In cancer treatment,
354 TNFAIP2 was chosen as one of the six signature genes predicting
355 chemotherapeutic and immunotherapeutic efficacies, with high-senescore
356 patients benefiting from immunotherapy and low-senescore patients
357 responsive to chemotherapy[50].
358 These reports provide apossible explanation for previous studies showing that
359 ITGB4 is important in EMT and cancer stemness. According to our results that
360 there isan interaction between ITGB4 and TNFAIP2, ITGB4 might regulate
361 EMT and stemness through TNFAIP2.TNFAIP2 is one of the important factors
362 induced by tumor necrosis factor alpha (TNFα). Interestingly, TNFα release
363 could be induced by therapeutic drugs from multiple tumor cell lines. The
364 acquisition of docetaxel resistance was accompanied by increased constitutive
365 production of TNFα[51]. In addition, TNFα is a key tumor-promoting effector
366 molecule secreted by tumor-associated macrophages. *In vitro* neutralizing
367 TNFα was observed to inhibit tumor progression and improve the curative
368 effect of bevacizumab[52]. Therefore, the mechanism by which TNFα plays a
369 role in chemotherapeutic resistance in breast cancer should be further
370 investigated. TNFα neutralizing provides novel opinions elucidating drug
371 resistance.
372 For future studies, it will be important to develop *Tnfaip2* knockout mice to

373 investigate the exact role of TNFAIP2 physiologically. According to recent
374 studies and our findings, agents targeting the interaction among
375 ITGB4/TNFAIP2/IQGAP1 would be a promising trend for developing drugs to
376 overcome the resistance phenomenon.
377
378 In summary, ITGB4 and TNFAIP2 play important roles in breast cancer
379 chemoresistance. TNFAIP2 activates Rac1 to promote chemoresistance
380 through IQGAP1. In addition, ITGB4 activates Rac1 through TNFAIP2 and
381 IQGAP1 and confer DNA damage drug resistance in TNBC (Figure 8 E).
382 These results indicate that the ITGB4/TNFAIP2/IQGAP1/Rac1 axis provides
383 potential therapeutic targets to overcome DNA damage drug resistance in
384 TNBC.
385

Data availability statement

The authors confirm that the data supporting the findings of this study are available within the article and its supplementary materials.

Acknowledgments

This work was supported by National Key R&D Program of China (2020YFA0112300), National Natural Science Foundation of China (81830087, U2102203, 81672624, 82102987, and 82203413), the Yunnan Fundamental Research Projects (202101AS070050), and the Guangdong Foundation Committee for Basic and Applied Basic Research projects (2022A1515012420).

Author contributions

H.F., W.R., Q.C., H.L. and C.Y. conducted different parts of the experiments. W.L., X.W., X.L. and Y.S. provided some advice about this project. C.C. and J.F. designed the study. C.C., J.F., and Y.S. supervised the study. H.F. wrote the original draft and W.R., Q.C., H.L., C.C. and J.F. reviewed and edited the draft.

Declaration of interests

The authors declare no conflicts of interest.

Figure titles and legends

Figure1. TNFAIP2 promotes TNBC DNA damage drug resistance

409 (A-E) Stable TNFAIP2 overexpression in HCC1806 and HCC1937 cells
410 significantly increased cell viability in the presence of EPI (0-1.6 μM) or BMN
411 (0-40 μM) treatment for 48h, as measured by the SRB assay. TNFAIP2 protein
412 expression was detected by WB.
413 (F-J) Stable TNFAIP2 knockdown in HCC1806 and HCC1937 cells
414 significantly decreased cell viability in the presence of EPI (0-1.6 μM) or BMN
415 (0-40 μM) treatment for 48h, as measured by the SRB assay. TNFAIP2 protein
416 expression was detected by WB.
417 (K) TNFAIP2 promoted DNA damage repair in the presence of EPI and BMN.
418 HCC1806 and HCC1937 cells stably overexpressing TNFAIP2 were treated
419 with 400 or 800 nM EPI for 48h and 10 μM BMN for 24h, respectively.
420 TNFAIP2, γH2AX, and PARP protein expression was detected by WB.
421 (L) TNFAIP2 knockdown increased DNA damage in the presence of EPI and
422 BMN. Stable TNFAIP2 knockdown cells were treated with 400 or 800 nM EPI
423 for 24 or 48h and 2.5 μM BMN for 24h. TNFAIP2, γH2AX, and PARP protein
424 expression was detected by WB.
425
426 **Figure2. TNFAIP2 confers TNBC drug resistance *in vivo***
427 (A-F) TNFAIP2 knockdown increased the sensitivity of HCC1806 breast
428 cancer cells to EPI and BMN *in vivo*. HCC1806 cells with stable TNFAIP2
429 knockdown were transplanted into the fat pad of 7-week-old female nude mice.
430 When the average tumor size reached approximately 50 mm^3 after inoculation,
431 mice in each group were randomly divided into two subgroups (n=4/group) to
432 receive EPI (2.5 mg/kg), BMN (1 mg/kg) or vehicle control for 23 or 29 days
433 (A-B). Tumor size was measured twice a week (C-D), and tumor masses were
434 collected and weighed at the end of the experiments (E-F). *: $P<0.05$, **:
435 $P<0.01$, *t*-test.
436
437 **Figure3. TNFAIP2 promotes TNBC drug resistance and DNA damage**
438 **repair via Rac1**

439 (A-F) Rac1 knockdown abolished TNFAIP2-induced TNBC resistance to EPI
440 and BMN. HCC1806 (A-C) and HCC1937 (D-F) cells with stable TNFAIP2
441 overexpression were transfected with Rac1 or control siRNA, followed by
442 treatment with EPI (0-1600 nM) and BMN (0-40 μM) for 48 or 72 h, respectively.
443 Cell viability was measured by the SRB assay. Protein expression levels were
444 analyzed by WB.
445 (G-J) Rac1 depletion abolished TNFAIP2-induced DNA damage decrease in
446 response to EPI and BMN. HCC1806 (G-H) and HCC1937 (I-J) cells with
447 stable TNFAIP2 overexpression were transfected with Rac1 or control siRNA,
448 followed by treatment with EPI (400 or 800 nM) and BMN (10 μM) for 24h,
449 respectively. Protein expression levels were analyzed by WB.
450
451 **Figure4. IQGAP1 mediates Rac1 activation by TNFAIP2 and promotes**
452 **TNBC drug resistance**
453 (A) The IP-MS result of TNFAIP2 in HCC1806 cells.
454 (B) Endogenous TNFAIP2 interacts with IQGAP1 in HCC1806 cells.
455 Endogenous TNFAIP2 protein was immunoprecipitated using ananti-IQGAP1
456 antibody. Immunoglobulin (Ig)G served as the negative control. Endogenous
457 TNFAIP2 was detected by WB.
458 (C-G) IQGAP1 knockdown in HCC1806 and HCC1937 cells significantly
459 decreased cell viability in the presence of EPI (0-1600 nM) and BMN (0-40 μM),
460 as measured by the SRB assay. IQGAP1 protein expression was detected by
461 WB.
462 (H) IQGAP1 knockdown in HCC1806 and HCC1937 cells increased DNA
463 damage of EPI and BMN. HCC1806 and HCC1937 cells with IQGAP1
464 knockdown were treated with 800 nM EPI for 24h and 10 μM BMN for24h,
465 respectively. ITGB4, γH2AX, and PARP protein expression was detected by
466 WB.
467 (I-K) IQGAP1 knockdown abolished TNFAIP2-confered resistance to EPI and
468 BMN. HCC1806 cells with stable TNFAIP2 overexpression were transfected

469 with IQGAP1 or control siRNA, followed by treatment with EPI (0-1600 nM)
470 and BMN (0-40 μM) for 48 or 72 h, respectively. Cell viability was measured by
471 the SRB assay. IQGAP1 protein expression was detected by WB.
472 (L) IQGAP1 knockdown abolished TNFAIP2-confered resistance to EPI and
473 BMN. HCC1806 and HCC1937 cells with stable TNFAIP2 overexpression
474 were transfected with IQGAP1 or control siRNA, followed by treatment with
475 EPI (800 nM) and BMN (10 μM) for 24h, respectively. Protein expression levels
476 were analyzed by WB.
477 (M) IQGAP1 knockdown abolished TNFAIP2-confered Rac1 activation.
478 HCC1806 and HCC1937 cells with stable TNFAIP2 overexpression were
479 transfected with IQGAP1 or control siRNA. GTP-Rac1 levels were assessed
480 using PAK-PBD beads.
481
482 **Figure5. ITGB4 interacts with TNFAIP2 and promotes TNBC drug**
483 **resistance and DNA damage repair**
484 (A) TNFAIP2 interacts with ITGB4.HCC1806 cells with stable TNFAIP2
485 overexpression were collected from flag-tagged TNFAIP2 cell lysates for
486 immunoprecipitation assays using Flag-M2 beads, and ITGB4 was detected by
487 WB.
488 (B) Endogenous TNFAIP2 interacts with ITGB4 in HCC1806 cells.
489 Endogenous TNFAIP2 protein was immunoprecipitated using an anti-TNFAIP2
490 antibody. IgG served as the negative control. Endogenous ITGB4 was
491 detected by WB.
492 (C) Endogenous ITGB4 interacts with TNFAIP2 in HCC1806 cells.
493 Endogenous ITGB4 protein was immunoprecipitated using an anti-ITGB4
494 antibody. IgG served as the negative control. Endogenous TNFAIP2 was
495 detected by WB.
496 (D-I) ITGB4 knockdown in HCC1806 and HCC1937 cells significantly
497 decreased cell viability in the presence of EPI (0-800 nM) and BMN (0-40 μM),
498 as measured by the SRB assay. ITGB4 protein expression was detected by

499 WB.

500 (J-N) ITGB4 depletion promotes HCC1806 breast cancer cell sensitivity to EPI
501 and BMN treatment *in vivo*. HCC1806 cells with stable ITGB4 knockdown were
502 transplanted into the fat pad of 7-week-old female nude mice. When the
503 average tumor size reached approximately 50 mm^3 after inoculation, the mice
504 in each group were randomly divided into two subgroups (n=4/group) to
505 receive EPI (2.5 mg/kg), BMN (1 mg/kg) or vehicle control for 22 days(J).
506 Tumor masses were collected and weighed at the end of the experiments(K),
507 and tumor size was measured twice a week (L-N).*: $P<0.05$, **: $P<0.01$, *t*-test.
508 (O) ITGB4 knockdown increased DNA damage of EPI and BMN. HCC1806
509 and HCC1937 cells with ITGB4 knockdown were treated with 400 nM EPI for
510 24h and 5 μM BMN for 24h, respectively. ITGB4, γH2AX, and PARP protein
511 expression was detected by WB.

512

513 **Figure6. ITGB4 activates Rac1 through TNFAIP2 and IQGAP1**

514 (A) Overexpression of ITGB4 increased GTP-Rac1 levels in HCC1806 and
515 HCC1937 cells. GTP-Rac1 were assessed using PAK-PBD beads.
516 (B) Knockdown of ITGB4 by shRNA decreased GTP-Rac1 levels in HCC1806
517 and HCC1937 cells.
518 (C-D) ITGB4 activates Rac1 through TNFAIP2. HCC1806 (C) and HCC1937
519 (D) cells with stable ITGB4 overexpression were transfected with TNFAIP2 or
520 control siRNA.
521 (E-F) ITGB4 activates Rac1 through IQGAP1.HCC1806 (E) and HCC1937 (F)
522 cells with stable ITGB4 overexpression were transfected with IQGAP1 or
523 control siRNA.

524

525 **Figure7. ITGB4 promotes TNBC drug resistance via**
526 **TNFAIP2/IQGAP1/Rac1**

527 (A-C) ITGB4 promotes TNBC drug resistance through TNFAIP2. TNFAIP2
528 knockdown abolished ITGB4-induced resistance to EPI and BMN. HCC1806

529 cells with stable ITGB4 overexpression were transfected with TNFAIP2 or
530 control siRNA, followed by treatment with EPI (0-400 nM) and BMN (0-30 μM)
531 for 48 or 72 h, respectively. Cell viability was measured by the SRB assay.
532 Protein expression levels were analyzed by WB.
533 (D-F) ITGB4 promotes TNBC drug resistance through IQGAP1. HCC1806
534 cells with stable ITGB4 overexpression were transfected with IQGAP1 or
535 control siRNA, followed by treatment with EPI (0-800 nM) and BMN (0-40 μM)
536 for 48 or 72 h, respectively. Cell viability was measured by the SRB assay.
537 Protein expression levels were analyzed by WB.
538 (G-I) ITGB4 promotes TNBC drug resistance through Rac1. HCC1806 cells
539 with stable ITGB4 overexpression were transfected with Rac1 or control siRNA,
540 followed by treatment with EPI (0-400 nM) and BMN (0-40 μM) for 48 or 72 h,
541 respectively. Cell viability was measured by the SRB assay. Protein expression
542 levels were analyzed by WB.
543 (J) ITGB4 promotes DNA damage repair through TNFAIP2. HCC1806 cells
544 with stable ITGB4 overexpression were transfected with TNFAIP2 or control
545 siRNA, followed by treatment with EPI (400 nM) and BMN (5 μM) for 24h.
546 Protein expression levels were analyzed by WB.
547 (K) ITGB4 promotes DNA damage repair through IQGAP1. HCC1806 cells
548 with stable ITGB4 overexpression were transfected with IQGAP1 or control
549 siRNA, followed by treatment with EPI (400 nM) and BMN (5 μM) for 24h.
550 Protein expression levels were analyzed by WB.
551 (L) ITGB4 promotes DNA damage repair through Rac1. HCC1806 cells with
552 stable ITGB4 overexpression were transfected with Rac1 or control siRNA,
553 followed by treatment with EPI (400 nM) and BMN (5 μM) for 24h. Protein
554 expression levels were analyzed by WB.
555
556 **Figure8. TNFAIP2 expression levels positively correlated with ITGB4 in**
557 **TNBC tissues**

558 Representative IHC images of TNFAIP2 and ITGB4 protein expression in
559 breast cancer tissues are shown. The final expression assessment was
560 performed by combining the two scores (0–2=low, 6–7=high). A and B indicate
561 low scores, C and D indicate high scores, and Figure E is the work model of
562 this paper.

563

564 **Table 1. The correlation of TNFAIP2 and ITGB4 protein expression levels**
565 **in human TNBC specimens.**

566

567 **STAR Methods**

568 **Cell lines and reagents**

569 All cell lines used in this study, including HCC1806, HCC1937, and HEK293T
570 cells, were purchased from ATCC (American Type Culture Collection,
571 Manassas, VA, USA) and validated by STR (short tandem repeat) analysis.
572 HCC1806 and HCC1937 cells were cultured in RPMI 1640 medium
573 supplemented with 5% FBS. HEK293T cells were cultured in DMEM (Thermo
574 Fisher, Grand Island, USA) with 5% FBS at 37°C with 5% CO_2. Epirubicin(EPI)
575 (Cat#HY-13624A),cisplatin(DDP)(Cat#HY-17394), talazoparib (BMN)
576 (Cat#HY-16106), and olaparib (AZD) (Cat#HY-10162) were purchased from
577 MCE (New Jersey, USA).

578

579 **Plasmid construction and stable TNFAIP2 and ITGB4 overexpression**

580 We constructed the full-length *TNFAIP2/ITGB4* gene and then subcloned them
581 into the pCDH lentiviral vector. The packaging plasmids (including

582 pMDLg/pRRE, pRSV-Rev, and pCMV-VSV-G) and pCDH-TNFAIP2/ITGB4
583 expression plasmid were cotransfected into HEK293T cells (2 ×10^6 in 10 cm
584 plate) to produce lentivirus. Following transfection for 48 h, the lentivirus was
585 collected and used to infect HCC1806 and HCC1937 cells. Forty-eight hours
586 later, puromycin (2 μg/ml) was used to screen the cell populations.
587

588 **Stable knockdown of TNFAIP2 and ITGB4**

589 The pSIH1-H1-puro shRNA vector was used to expressTNFAIP2, ITGB4 and
590 luciferase(LUC)shRNAs.TNFAIP2shRNA#1,5'-GACUUGGGCUCACAGAUAA
591 -3';TNFAIP2shRNA#2,5'-GAUUGAGGUGGCCACUUAU-3';ITGB4shRNA#1,5'
592 -ACGACAGCTTCCTTATGTA-3';ITGB4shRNA#2,5'-CAGCGACTACACTATTG
593 GA-3';LuciferaseshRNA,5'-CUUACGCUGAGUACUUCGA-3'; HCC1806 and
594 HCC1937 cells were infected with lentivirus. Stable populations were selected
595 using 1 to 2 mg/mL puromycin. The knockdown effect was evaluated by
596 Western blotting.
597

598 **RNA interference**

599 The siRNA target sequences used in this study are as follows:
600 TNFAIP2siRNA#1,5'-GACUUGGGCUCACAGAUAA-3';TNFAIP2siRNA#2,5'-
601 GAUUGAGGUGGCCACUUAU-3';ITGB4siRNA#1,5'-ACGACAGCTTCCTTAT
602 GTA-3';ITGB4siRNA#2,5'-CAGCGACTACACTATTGGA-3';Rac1siRNA,5'-CG
603 GCACCACUGUCCCAACA-3';IQGAP1siRNA#1,5'-GCAGGTGGATTACTATAA

604 A-3';IQGAP1siRNA#2,5'-CUAGUGAAACUGCAACAGA-3'. All siRNAs were
605 synthesized by RiboBio (RiboBio, China) and transfected at a final
606 concentration of 50 nM.
607
608 **Antibodies and Western blotting (WB)**
609 The WB procedure has been described in our previous study[53]. Anti-TNFAIP2
610 (sc-28318), anti-ITGB4 (sc-9090) and anti-GAPDH (sc-25778) antibodies were
611 purchased from Santa Cruz Biotechnology (Santa Cruz, CA, USA). The
612 anti-PARP (#9542) antibody was purchased from CST. Anti-Rac1 (05–389)
613 and anti-γH2AX (3475627) antibodies were purchased from Millipore (Billerica,
614 MA, USA). Anti-β-actin (A5441) and anti-Tubulin (T5168) antibodies were
615 purchased from Sigma–Aldrich (St Louis, MO, USA).The anti-IQGAP1
616 (ab86064) antibody was purchased from Abcam.
617
618 **Immunopurification and silver staining**
619 Immunoprecipitation and silver staining lysates from HCC1806 cells stably
620 expressing Flag-TNFAIP2 were prepared by incubating the cells in lysis buffer
621 containing a protease inhibitor cocktail (MCE). Cell lysates were obtained from
622 approximately 2.5×10^{8} cells, and after binding with anti-Flag M2 affinity gel
623 (Sigma) for 2 h as recommended by the manufacturer, the affinity gel was
624 washed with cold lysis plus 0.2% NP-40. FLAG peptide (Sigma) was applied to
625 elute the Flag-labeled protein complex as described by the vendor. The elutes

626 were collected and visualized on NuPAGE 4%-12% Bis-Trisgels (Invitrogen,
627 CA, USA) followed by silver staining with a silver staining kit (Pierce, Illinois,
628 USA). The distinct protein bands were retrieved and analyzed by LC–Mass.
629

630 **Immunoprecipitation and GST pull-down**

631 For exogenous interaction between ITGB4 and Flag-TNFAIP2, cell lysates
632 were directly incubated with anti-Flag M2 affinity gel (A2220; Sigm) overnight
633 at 4°C. For endogenous protein interaction, cell lysates were first incubated
634 with anti-TNFAIP2/ITGB4/IQGAP1 antibodies or mouse IgG/rabbit IgG
635 (sc-2028; Santa Cruz Biotechnology, CA, USA) and then incubated with
636 Protein A/G plusagarose beads (sc-2003; Santa Cruz BiotechnologyFor the
637 GST pulldown assay, cell lysates were directly incubated with
638 GlutathioneSepharose 4B (52-2303-00; GE Healthcare) overnight at 4°C. The
639 precipitates were washed four times with 1 ml of lysis buffer, boiled for 10
640 minutes with 1×SDS sample buffer, and subjected to WB analysis.
641

642 **Cell viability assays**

643 Cell viability was measured by SRB assays as described in our previous
644 study[54].Cell viability was measured by SRB assays. Briefly, cells were seeded
645 in 96-well plates. Then, the cells were cultured for the indicated timeand fixed
646 with 10% trichloroacetic acid at room temperature for30 min, followed by
647 incubation with 0.4% SRB (w/v) solution in 1% acetic acid for 20 min at room

648 temperature. Finally, SRB was dissolved in 10 mM unbuffered Tris base, and
649 the absorbance was measured at a wavelength of 530 nm on a plate reader
650 (Bio Tek, Vermont, USA).
651
652 **Rac1 activation assays**
653 Rac1 activation was examined using the Cdc42 Activation Assay Biochem Kit
654 (BK034, Cytoskeleton, Denver, USA) following them anufacturer's instructions.
655 Cells were harvested with cell lysis buffer, and1 mg of protein lysate in a 1 ml
656 total volume at 4°C was immediately precipitated with 10 μg of PAK-PBD
657 beads for 60 min with rotation. After washing three times with wash buffer,
658 agarose beads were resuspended in 30 μl of 2×SDS sample buffer and boiled
659 for 5 min. Rac1-GTP was examined by WB with an anti-Rac1 antibody.
660
661 **Xenograft experiments**
662 We purchased 6- to 7-week-old female BALB/c nude mice from SLACCAS
663 (Changsha, China). Animal feeding and experiments were approved by the
664 animal ethics committee of Kunming Institute of Zoology, Chinese Academy of
665 Sciences. HCC1806-shLuc, HCC1806-shTNFAIP2, or HCC1806-shITGB4
666 cells (1×10^6 in Matrigel (BD Biosciences, NY, USA)) were implanted into the
667 mammary fat pads of the mice. When the tumor volume reached
668 approximately 50 mm^3, the nude mice were randomly assigned to the control
669 and treatment groups (n = 4/group). EPI, BMN, and DDP were dissolved in

670 ddH_2O. The control group was given vehicle alone, and the treatment group
671 received EPI (2.5 mg/kg), BMN (1 mg/kg), and DDP (2.5 mg/kg) alone via
672 intraperitoneal injection every three days for 18 or 27 days. The tumor volume
673 was calculated as follows: tumor volume was calculated by the formula: ($\pi\times$
674 length × $width^2$)/6.
675

676 **Immunohistochemical staining**

677 Paraffin-embedded clinical TNBC specimens were obtained from the First
678 Affiliated Hospital, Zhengzhou University, Zhengzhou, China. Informed
679 consent was obtained from all subjects. Two tissue microarrays containing 135
680 TNBC breast cancer tissues were constructed. For the immunohistochemistry
681 (IHC) assay, the slides were deparaffinized, rehydrated, and pressure cooker
682 heated for 2.5 min in EDTA for antigen retrieval. Endogenous peroxidase
683 activity was inactivated by adding an endogenous peroxidase blocker
684 (OriGene, China) for 15 min at room temperature. Slides were incubated
685 overnight at 4°Cwith anti-TNFAIP2 (1:200) or anti-ITGB4 (1:500). After 12 h,
686 the slides were washed three times with PBS and incubated with secondary
687 antibodies (hypersensitive enzyme-labeled goat anti-mouse/rabbit IgG
688 polymer (OriGene, China) at room temperature for 20 min, DAB concentrate
689 chromogenic solution (1:200dilution of concentrated DAB chromogenic
690 solution), counterstained with 0.5% hematoxylin, dehydrated with graded
691 concentrations of ethanol for 3 min each (70%–80%–90%–100%),and finally

692 stained with dimethyl benzene immunostainedslides were evaluated by light
693 microscopy. The IHC signal was scored using the 'Allred Score' method.
694

695 **Statistical analysis**

696 All graphs were created using GraphPad Prism software version 5.0.
697 Comparisons between two independent groups were assessed by two-tailed
698 Student's t-test. One-way analysis of variance with least significant differences
699 was used for multiple group comparisons. *P*-values of <0.05, 0.01 or 0.001
700 were considered to indicate a statistically significant result, comparisons
701 significant at the 0.05 level are indicated by*, at the 0.01 level are indicated by
702 **, or at the 0.001 level are indicated by ***.
703

704 **Supplemental information titles and legends**

705 **FigureS1. TNFAIP2 promotes TNBC DNA damage drug resistance**
706 (A-E) Stable TNFAIP2 overexpression in HCC1806 and HCC1937 cells
707 significantly increased cell viability in the presence of DDP (0-40 μM) or AZD
708 (0-40 μM) treatment for 48h, as measured by the SRB assay. TNFAIP2 protein
709 expression was detected by WB.
710 (F-J) Stable TNFAIP2 knockdown in HCC1806 and HCC1937 cells
711 significantly decreased cell viability in the presence of DDP (0-40 μM) or AZD
712 (0-40 μM) treatment for 48h, as measured by the SRB assay. TNFAIP2 protein
713 expression was detected by WB.
714 (K) TNFAIP2 promoted DNA damage repair in the presence of DDP and AZD.
715 HCC1806 and HCC1937 cells stably overexpressing TNFAIP2 were treated
716 with 20 μM DDP for 24 h or 48h and 10 μM AZD for 24h, respectively. TNFAIP2,

γH2AX, and PARP protein expression was detected by WB.

(L) TNFAIP2 knockdown increased DNA damage in the presence of DDP and AZD. Stable TNFAIP2 knockdown cells were treated with 2.5 or 20 μM DDP for 24h and 2.5 μM AZD for 24h. TNFAIP2, γH2AX, and PARP protein expression was detected by WB.

FigureS2. TNFAIP2 confers TNBC drug resistance *in vivo*

(A-F) TNFAIP2 knockdown increased the sensitivity of HCC1806 breast cancer cells to DDP *in vivo*. HCC1806 cells with stable TNFAIP2 knockdown were transplanted into the fat pad of 7-week-old female nude mice. When the average tumor size reached approximately 50 mm^3 after inoculation, mice in each group were randomly divided into two subgroups (n=4/group) to receive DDP (2.5 mg/kg) or vehicle control for 23 days (A). Tumor size was measured twice a week (B), tumor masses were collected and weighed at the end of the experiments (C), and mouse masses were collected and weighed at the beginning or end of the experiments (D-F). *: $P<0.05$, **: $P<0.01$, *t*-test.

FigureS3. TNFAIP2 promotes TNBC drug resistance and DNA damage repair via Rac1

(A-F) Rac1 knockdown abolished TNFAIP2-induced TNBC resistance to DDP and AZD. HCC1806 (A-C) and HCC1937 (D-F) cells with stable TNFAIP2 overexpression were transfected with Rac1 or control siRNA, followed by treatment with DDP (0-40 μM) and AZD (0-40 μM) for 48 or 72 h, respectively. Cell viability was measured by the SRB assay. Protein expression levels were analyzed by WB.

(G-J) Rac1 depletion abolished TNFAIP2-induced DNA damage decrease in response to DDP and AZD. HCC1806 (G-H) and HCC1937 (I-J) cells with stable TNFAIP2 overexpression were transfected with Rac1 or control siRNA, followed by treatment with DDP (20 μM) and AZD (10 μM) for 24h, respectively. Protein expression levels were analyzed by WB.

747

748 **FigureS4. IQGAP1 mediates Rac1 activation by TNFAIP2 and promotes**
749 **TNBC drug resistance**

750 (A) TNFAIP2 interacts with IQGAP1. HCC1806 cells with stable TNFAIP2
751 overexpression were collected from flag-tagged TNFAIP2 cell lysates for
752 immunoprecipitation assays using Flag-M2 beads, and IQGAP1 was detected
753 by WB.

754 (B) Mapping the domains of TNFAIP2 that interact with IQGAP1. Flag-tagged
755 full-length or truncated TNFAIP2 was transfected into HEK293T cells with
756 no-tagged full-length IQGAP1. Cell lysates were collected for
757 immunoprecipitation using Flag-M2 beads, and IQGAP1 was detected by WB.

758 (C-E) IQGAP1 knockdown abolished TNFAIP2-confered resistance to EPI and
759 BMN. HCC1937 cells with stable TNFAIP2 overexpression were transfected
760 with IQGAP1 or control siRNA, followed by treatment with EPI (0-1600 nM)
761 and BMN (0-40 μM) for 48 or 72 h, respectively. Cell viability was measured by
762 the SRB assay, and IQGAP1 was detected by WB.

763

764 **FigureS5. ITGB4 interacts with TNFAIP2 and promotes TNBC drug**
765 **resistance and DNA damage repair**

766 (A-F) ITGB4 knockdown in HCC1806 and HCC1937 cells significantly
767 decreased cell viability in the presence of DDP (0-40 μM) and AZD (0-40 μM),
768 as measured by the SRB assay. ITGB4 protein expression was detected by
769 WB.

770 (G) ITGB4 knockdown increased DNA damage of DDP and AZD. HCC1806
771 and HCC1937 cells with ITGB4 knockdown were treated with 5μM or 7.5 μM
772 DDP for 24h and 15 μM or 20 μM AZD for 24h, respectively. ITGB4, γH2AX,
773 and PARP protein expression was detected by WB.

774 (H) Mouse masses were collected and weighed at the end of the experiments.

775 (I) The model of full-length or truncated TNFAIP2.

776 (J) Mapping the domains of TNFAIP2 that interact with ITGB4. GST-tagged

Full-length ITGB4 was transfected into HEK293T cells with flag-tagged full-length or truncated TNFAIP2. TNFAIP2 protein was immunoprecipitated usingFlag-M2 beads, and ITGB4 was detected by WB.

(K) Mapping the domains of TNFAIP2 that interact with ITGB4. No-tagged full-length ITGB4 was transfected into HEK293T cells with GST-tagged full-length or truncated TNFAIP2. Cell lysates were collected for the GST pull-down assay, and ITGB4 was detected by WB.

(L) The model of full-length or truncated ITGB4.

(M) Mapping the domains of ITGB4 that interact with TNFAIP2. Flag-tagged full-length TNFAIP2 was transfected into HEK293T cells with no-tagged full-length or truncated ITGB4. Cell lysates were collected for immunoprecipitation using Flag-M2 beads, and ITGB4 was detected by WB.

FigureS6. ITGB4 promotes TNBC drug resistance via TNFAIP2/IQGAP1/Rac1

(A-F) ITGB4 promotes TNBC drug resistance through TNFAIP2. TNFAIP2 knockdown abolished ITGB4-induced resistance to DDP and AZD. HCC1806 (A-C) and HCC1937 (D-F) cells with stable ITGB4 overexpression were transfected with TNFAIP2 or control siRNA, followed by treatment with DDP (0-30 μM) and AZD (0-30 μM) for 48 or 72h, respectively. Cell viability was measured by the SRB assay. Protein expression levels were analyzed by WB.

(G-L) ITGB4 promotes TNBC drug resistance through Rac1. Rac1 knockdown abolished ITGB4-induced resistance to DDP and AZD. HCC1806 (G-I) and HCC1937 (J-L) cells with stable ITGB4 overexpression were transfected with Rac1 or control siRNA, followed by treatment with DDP (0-20 μM) and AZD (0-40 μM) for 48 or 72h, respectively. Cell viability was measured by the SRB assay. Protein expression levels were analyzed by WB.

(M) ITGB4 promotes DNA damage repair through TNFAIP2. HCC1806 and HCC1937 cells with stable ITGB4 overexpression were transfected with TNFAIP2 or control siRNA, followed by treatment with DDP (7.5 μM or 10 μM)

807 and AZD (20 μM or 30 μM) for 24h. Protein expression levels were analyzed
808 by WB.
809 (N) ITGB4 promotes DNA damage repair through Rac1. HCC1806 and
810 HCC1937 cells with stable ITGB4 overexpression were transfected with Rac1
811 or control siRNA, followed by treatment with DDP (7.5 μM) and AZD (20 μM or
812 30 μM) for 24h. Protein expression levels were analyzed by WB.
813 (O-Q) ITGB4 promotes TNBC drug resistance through TNFAIP2. TNFAIP2
814 knockdown abolished ITGB4-induced resistance to EPI and BMN. HCC1937
815 cells with stable ITGB4 overexpression were transfected with TNFAIP2 or
816 control siRNA, followed by treatment with EPI (0-800 nM) and BMN (0-30 μM)
817 for 48 or 72 h, respectively. Cell viability was measured by the SRB assay.
818 Protein expression levels were analyzed by WB.
819 (R-T) ITGB4 promotes TNBC drug resistance through IQGAP1. HCC1937
820 cells with stable ITGB4 overexpression were transfected with IQGAP1 or
821 control siRNA, followed by treatment with EPI (0-800 nM) and BMN (0-40 μM)
822 for 48 or 72 h, respectively. Cell viability was measured by the SRB assay.
823 Protein expression levels were analyzed by WB.
824 (U-W) ITGB4 promotes TNBC drug resistance through Rac1. HCC1937 cells
825 with stable ITGB4 overexpression were transfected with Rac1 or control siRNA,
826 followed by treatment with EPI (0-800 nM) and BMN (0-30 μM) for 48 or 72 h,
827 respectively. Cell viability was measured by the SRB assay. Protein expression
828 levels were analyzed by WB.
829 (X) ITGB4 promotes DNA damage repair through TNFAIP2. HCC1937 cells
830 with stable ITGB4 overexpression were transfected with TNFAIP2 or control
831 siRNA, followed by treatment with EPI (800 nM) and BMN (10 μM) for 24h.
832 Protein expression levels were analyzed by WB.
833 (Y) ITGB4 promotes DNA damage repair through IQGAP1. HCC1937 cells
834 with stable ITGB4 overexpression were transfected with IQGAP1 or control
835 siRNA, followed by treatment with EPI (800 nM) and BMN (10 μM) for 24h.
836 Protein expression levels were analyzed by WB.

(Z) ITGB4 promotes DNA damage repair through Rac1. HCC1937 cells with stable ITGB4 overexpression were transfected with Rac1 or control siRNA, followed by treatment with EPI (800 nM) and BMN (10 μM) for 24h. Protein expression levels were analyzed by WB.

References

1. Bray, F., Ferlay, J., Soerjomataram, I., Siegel, R.L., Torre, L.A., and Jemal, A. (2018). Global cancer statistics 2018: GLOBOCAN estimates of incidence and mortality worldwide for 36 cancers in 185 countries. CA: a cancer journal for clinicians *68*, 394-424. 10.3322/caac.21492.
2. Zhao, S., Ma, D., Xiao, Y., Li, X.M., Ma, J.L., Zhang, H., Xu, X.L., Lv, H., Jiang, W.H., Yang, W.T., et al. (2020). Molecular Subtyping of Triple-Negative Breast Cancers by Immunohistochemistry: Molecular Basis and Clinical Relevance. *25*, e1481-e1491. 10.1634/theoncologist.2019-0982.
3. Sotiriou, C., and Pusztai, L. (2009). Gene-expression signatures in breast cancer. The New England journal of medicine *360*, 790-800. 10.1056/NEJMra0801289.
4. Bai, X., Ni, J., Beretov, J., Graham, P., and Li, Y. (2021). Triple-negative breast cancer therapeutic resistance: Where is the Achilles' heel? Cancer letters *497*, 100-111. 10.1016/j.canlet.2020.10.016.
5. Jamdade, V.S., Sethi, N., Mundhe, N.A., Kumar, P., Lahkar, M., and Sinha, N. (2015). Therapeutic targets of triple-negative breast cancer: a review. British journal of pharmacology *172*, 4228-4237. 10.1111/bph.13211.
6. Hill, D.P., Harper, A., Malcolm, J., McAndrews, M.S., Mockus, S.M., Patterson, S.E., Reynolds, T., Baker, E.J., Bult, C.J., Chesler, E.J., and Blake, J.A. (2019). Cisplatin-resistant triple-negative breast cancer subtypes: multiple mechanisms of resistance. BMC cancer *19*, 1039. 10.1186/s12885-019-6278-9.
7. Longley, D.B., and Johnston, P.G. (2005). Molecular mechanisms of drug resistance. The Journal of pathology *205*, 275-292. 10.1002/path.1706.
8. Rincón, R., Zazo, S., Chamizo, C., Manso, R., González-Alonso, P., Martín-Aparicio, E., Cristóbal, I., Cañadas, C., Perona, R., Lluch, A., et al. (2016). c-Jun N-Terminal Kinase Inactivation by Mitogen-Activated Protein Kinase Phosphatase 1 Determines Resistance to Taxanes and Anthracyclines in Breast Cancer. Molecular cancer therapeutics *15*, 2780-2790. 10.1158/1535-7163.mct-15-0920.
9. Jia, L., Zhou, Z., Liang, H., Wu, J., Shi, P., Li, F., Wang, Z., Wang, C., Chen, W., Zhang, H., et al. (2016). KLF5 promotes breast cancer proliferation, migration and invasion in part by upregulating the transcription of TNFAIP2. Oncogene *35*, 2040-2051. 10.1038/onc.2015.263.
10. Chen, L.C., Chen, C.C., Liang, Y., Tsang, N.M., Chang, Y.S., and Hsueh, C. (2011). A novel role for TNFAIP2: its correlation with invasion and metastasis in nasopharyngeal carcinoma. Modern pathology : an official journal of the United States and Canadian Academy of Pathology, Inc *24*, 175-184. 10.1038/modpathol.2010.193.
11. Cheng, Z., Wang, H.Z., Li, X., Wu, Z., Han, Y., Li, Y., Chen, G., Xie, X., Huang, Y., Du, Z., and Zhou, Y. (2015). MicroRNA-184 inhibits cell proliferation and invasion, and specifically targets TNFAIP2 in Glioma. Journal of experimental & clinical cancer research : CR *34*, 27.

879 10.1186/s13046-015-0142-9.
880 12. Niwa, N., and Tanaka, N. (2019). TNFAIP2 expression induces epithelial-to-mesenchymal
881 transition and confers platinum resistance in urothelial cancer cells. *99*, 1702-1713.
882 10.1038/s41374-019-0285-y.
883 13. Xie, Y., and Wang, B. (2017). Downregulation of TNFAIP2 suppresses proliferation and
884 metastasis in esophageal squamous cell carcinoma through activation of the Wnt/β-catenin
885 signaling pathway. Oncology reports *37*, 2920-2928. 10.3892/or.2017.5557.
886 14. Jia, L., Shi, Y., Wen, Y., Li, W., Feng, J., and Chen, C. (2018). The roles of TNFAIP2 in cancers and
887 infectious diseases. *22*, 5188-5195. 10.1111/jcmm.13822.
888 15. Didsbury, J., Weber, R.F., Bokoch, G.M., Evans, T., and Snyderman, R. (1989). rac, a novel
889 ras-related family of proteins that are botulinum toxin substrates. The Journal of biological
890 chemistry *264*, 16378-16382.
891 16. Rul, W., Zugasti, O., Roux, P., Peyssonnaux, C., Eychene, A., Franke, T.F., Lenormand, P., Fort, P.,
892 and Hibner, U. (2002). Activation of ERK, controlled by Rac1 and Cdc42 via Akt, is required for
893 anoikis. Annals of the New York Academy of Sciences *973*, 145-148.
894 10.1111/j.1749-6632.2002.tb04624.x.
895 17. Liu, W., Han, J., Shi, S., Dai, Y., and He, J. (2019). TUFT1 promotes metastasis and
896 chemoresistance in triple negative breast cancer through the TUFT1/Rab5/Rac1 pathway.
897 Cancer cell international *19*, 242. 10.1186/s12935-019-0961-4.
898 18. Yan, Y., Greer, P.M., Cao, P.T., Kolb, R.H., and Cowan, K.H. (2012). RAC1 GTPase plays an
899 important role in γ-irradiation induced G2/M checkpoint activation. Breast cancer research :
900 BCR *14*, R60. 10.1186/bcr3164.
901 19. Wu, M., Li, L., Hamaker, M., Small, D., and Duffield, A.S. (2019). FLT3-ITD cooperates with
902 Rac1 to modulate the sensitivity of leukemic cells to chemotherapeutic agents via regulation
903 of DNA repair pathways. Haematologica *104*, 2418-2428. 10.3324/haematol.2018.208843.
904 20. Hu, H., Juvekar, A., Lyssiotis, C.A., Lien, E.C., Albeck, J.G., Oh, D., Varma, G., Hung, Y.P., Ullas, S.,
905 Lauring, J., et al. (2016). Phosphoinositide 3-Kinase Regulates Glycolysis through Mobilization
906 of Aldolase from the Actin Cytoskeleton. Cell *164*, 433-446. 10.1016/j.cell.2015.12.042.
907 21. Li, Q., Qin, T., Bi, Z., Hong, H., Ding, L., Chen, J., Wu, W., Lin, X., Fu, W., Zheng, F., and Yao, Y.
908 (2020). Rac1 activates non-oxidative pentose phosphate pathway to induce chemoresistance
909 of breast cancer. *11*, 1456. 10.1038/s41467-020-15308-7.
910 22. Hervieu, A., and Heuss, S.F. (2020). A PI3K- and GTPase-independent Rac1-mTOR mechanism
911 mediates MET-driven anchorage-independent cell growth but not migration. *13*.
912 10.1126/scisignal.aba8627.
913 23. Li, Y., Li, P., and Wang, N. (2021). Effect of let-7c on the PI3K/Akt/FoxO signaling pathway in
914 hepatocellular carcinoma. Oncology letters *21*, 96. 10.3892/ol.2020.12357.
915 24. Feng, Y.X., Zhao, J.S., Li, J.J., Wang, T., Cheng, S.Q., Yuan, Y., Wang, F., Wang, X.F., and Xie, D.
916 (2010). Liver cancer: EphrinA2 promotes tumorigenicity through Rac1/Akt/NF-kappaB
917 signaling pathway. Hepatology (Baltimore, Md.) *51*, 535-544. 10.1002/hep.23313.
918 25. Higuchi, M., Onishi, K., Kikuchi, C., and Gotoh, Y. (2008). Scaffolding function of PAK in the
919 PDK1-Akt pathway. Nature cell biology *10*, 1356-1364. 10.1038/ncb1795.
920 26. Hu, F., Li, N., Li, Z., Zhang, C., Yue, Y., Liu, Q., Chen, L., Bilan, P.J., and Niu, W. (2018). Electrical
921 pulse stimulation induces GLUT4 translocation in a Rac-Akt-dependent manner in C2C12
922 myotubes. FEBS letters *592*, 644-654. 10.1002/1873-3468.12982.

923 27. Hamill, K.J., Hopkinson, S.B., DeBiase, P., and Jones, J.C. (2009). BPAG1e maintains
924 keratinocyte polarity through beta4 integrin-mediated modulation of Rac1 and cofilin
925 activities. Molecular biology of the cell *20*, 2954-2962. 10.1091/mbc.e09-01-0051.
926 28. Wu, J., Zhao, R., Lin, J., and Liu, B. (2018). Integrin β4 reduces DNA damage-induced p53
927 activation in colorectal cancer. Oncology reports *40*, 2183-2192. 10.3892/or.2018.6628.
928 29. Bierie, B., Pierce, S.E., Kroeger, C., Stover, D.G., Pattabiraman, D.R., Thiru, P., Liu Donaher, J.,
929 Reinhardt, F., Chaffer, C.L., Keckesova, Z., and Weinberg, R.A. (2017). Integrin-β4 identifies
930 cancer stem cell-enriched populations of partially mesenchymal carcinoma cells. Proceedings
931 of the National Academy of Sciences of the United States of America *114*, E2337-e2346.
932 10.1073/pnas.1618298114.
933 30. Ruan, S., Lin, M., Zhu, Y., Lum, L., Thakur, A., Jin, R., Shao, W., Zhang, Y., Hu, Y., Huang, S., et al.
934 (2020). Integrin β4-Targeted Cancer Immunotherapies Inhibit Tumor Growth and Decrease
935 Metastasis. Cancer research *80*, 771-783. 10.1158/0008-5472.can-19-1145.
936 31. Kang, S., Jang, Y., Chae, Y.C., and Kim, B.G.
937 32. Kim, B.G., Gao, M.Q., Choi, Y.P., Kang, S., Park, H.R., Kang, K.S., and Cho, N.H. (2012). Invasive
938 breast cancer induces laminin-332 upregulation and integrin β4 neoexpression in
939 myofibroblasts to confer an anoikis-resistant phenotype during tissue remodeling. Breast
940 cancer research : BCR *14*, R88. 10.1186/bcr3203.
941 33. Cherfils, J., and Zeghouf, M. (2013). Regulation of small GTPases by GEFs, GAPs, and GDIs.
942 Physiological reviews *93*, 269-309. 10.1152/physrev.00003.2012.
943 34. Schmidt, V.A. (2012). Watch the GAP: Emerging Roles for IQ Motif-Containing
944 GTPase-Activating Proteins IQGAPs in Hepatocellular Carcinoma. International journal of
945 hepatology *2012*, 958673. 10.1155/2012/958673.
946 35. Smith, J.M., Hedman, A.C., and Sacks, D.B. (2015). IQGAPs choreograph cellular signaling
947 from the membrane to the nucleus. Trends in cell biology *25*, 171-184.
948 10.1016/j.tcb.2014.12.005.
949 36. Gorisse, L., Li, Z., Wagner, C.D., Worthylake, D.K., Zappacosta, F., Hedman, A.C., Annan, R.S.,
950 and Sacks, D.B. (2020). Ubiquitination of the scaffold protein IQGAP1 diminishes its
951 interaction with and activation of the Rho GTPase CDC42. *295*, 4822-4835.
952 10.1074/jbc.RA119.011491.
953 37. Woods, D., and Turchi, J.J. (2013). Chemotherapy induced DNA damage response:
954 convergence of drugs and pathways. Cancer biology & therapy *14*, 379-389.
955 10.4161/cbt.23761.
956 38. Cheung-Ong, K., Giaever, G., and Nislow, C. (2013). DNA-damaging agents in cancer
957 chemotherapy: serendipity and chemical biology. Chemistry & biology *20*, 648-659.
958 10.1016/j.chembiol.2013.04.007.
959 39. Kim, C., Gao, R., Sei, E., Brandt, R., Hartman, J., Hatschek, T., Crosetto, N., Foukakis, T., and
960 Navin, N.E. (2018). Chemoresistance Evolution in Triple-Negative Breast Cancer Delineated by
961 Single-Cell Sequencing. Cell *173*, 879-893.e813. 10.1016/j.cell.2018.03.041.
962 40. Noordermeer, S.M., and van Attikum, H. (2019). PARP Inhibitor Resistance: A Tug-of-War in
963 BRCA-Mutated Cells. Trends in cell biology *29*, 820-834. 10.1016/j.tcb.2019.07.008.
964 41. Geenen, J.J.J., Linn, S.C., Beijnen, J.H., and Schellens, J.H.M. (2018). PARP Inhibitors in the
965 Treatment of Triple-Negative Breast Cancer. Clinical pharmacokinetics *57*, 427-437.
966 10.1007/s40262-017-0587-4.

42. Lee, A., and Djamgoz, M.B.A. (2018). Triple negative breast cancer: Emerging therapeutic modalities and novel combination therapies. Cancer treatment reviews *62*, 110-122. 10.1016/j.ctrv.2017.11.003.
43. Campbell, P.S., Mavingire, N., Khan, S., Rowland, L.K., Wooten, J.V., Opoku-Agyeman, A., Guevara, A., Soto, U., Cavalli, F., Loaiza-Pérez, A.I., et al. (2018). AhR ligand aminoflavone suppresses α6-integrin-Src-Akt signaling to attenuate tamoxifen resistance in breast cancer cells. *234*, 108-121. 10.1002/jcp.27013.
44. Ali, H.R., Dawson, S.J., Blows, F.M., Provenzano, E., Pharoah, P.D., and Caldas, C. (2011). Cancer stem cell markers in breast cancer: pathological, clinical and prognostic significance. Breast cancer research : BCR *13*, R118. 10.1186/bcr3061.
45. Friedland, J.C., Lakins, J.N., Kazanietz, M.G., Chernoff, J., Boettiger, D., and Weaver, V.M. (2007). alpha6beta4 integrin activates Rac-dependent p21-activated kinase 1 to drive NF-kappaB-dependent resistance to apoptosis in 3D mammary acini. Journal of cell science *120*, 3700-3712. 10.1242/jcs.03484.
46. Wei, T., and Lambert, P.F. (2021). Role of IQGAP1 in Carcinogenesis. *13*. 10.3390/cancers13163940.
47. Huang, L., Xu, S., Hu, D., Lu, W., Xie, X., and Cheng, X. (2015). IQGAP1 Is Involved in Enhanced Aggressive Behavior of Epithelial Ovarian Cancer Stem Cell-Like Cells During Differentiation. International journal of gynecological cancer : official journal of the International Gynecological Cancer Society *25*, 559-565. 10.1097/igc.0000000000000394.
48. Deb, S., Felix, D.A., and Koch, P. (2021). Tnfaip2/exoc3-driven lipid metabolism is essential for stem cell differentiation and organ homeostasis. *22*, e49328. 10.15252/embr.201949328.
49. Barutta, F., and Bellini, S. (2022). Protective effect of the tunneling nanotube-TNFAIP2/M-sec system on podocyte autophagy in diabetic nephropathy. 1-20. 10.1080/15548627.2022.2080382.
50. Zhou, L., Niu, Z., Wang, Y., Zheng, Y., Zhu, Y., Wang, C., Gao, X., Gao, L., and Zhang, W. (2022). Senescence as a dictator of patient outcomes and therapeutic efficacies in human gastric cancer. *8*, 13. 10.1038/s41420-021-00769-6.
51. Guo, F., and Yuan, Y. (2020). Tumor Necrosis Factor Alpha-Induced Proteins in Malignant Tumors: Progress and Prospects. *13*, 3303-3318. 10.2147/ott.s241344.
52. Liu, Y., Ji, X., Kang, N., Zhou, J., Liang, X., Li, J., Han, T., Zhao, C., and Yang, T. (2020). Tumor necrosis factor α inhibition overcomes immunosuppressive M2b macrophage-induced bevacizumab resistance in triple-negative breast cancer. Cell death & disease *11*, 993. 10.1038/s41419-020-03161-x.
53. Chen, C., Sun, X., Ran, Q., Wilkinson, K.D., Murphy, T.J., Simons, J.W., and Dong, J.T. (2005). Ubiquitin-proteasome degradation of KLF5 transcription factor in cancer and untransformed epithelial cells. Oncogene *24*, 3319-3327. 10.1038/sj.onc.1208497.
54. Chen, C., Zhou, Z., Ross, J.S., Zhou, W., and Dong, J.T. (2007). The amplified WWP1 gene is a potential molecular target in breast cancer. International journal of cancer *121*, 80-87. 10.1002/ijc.22653.

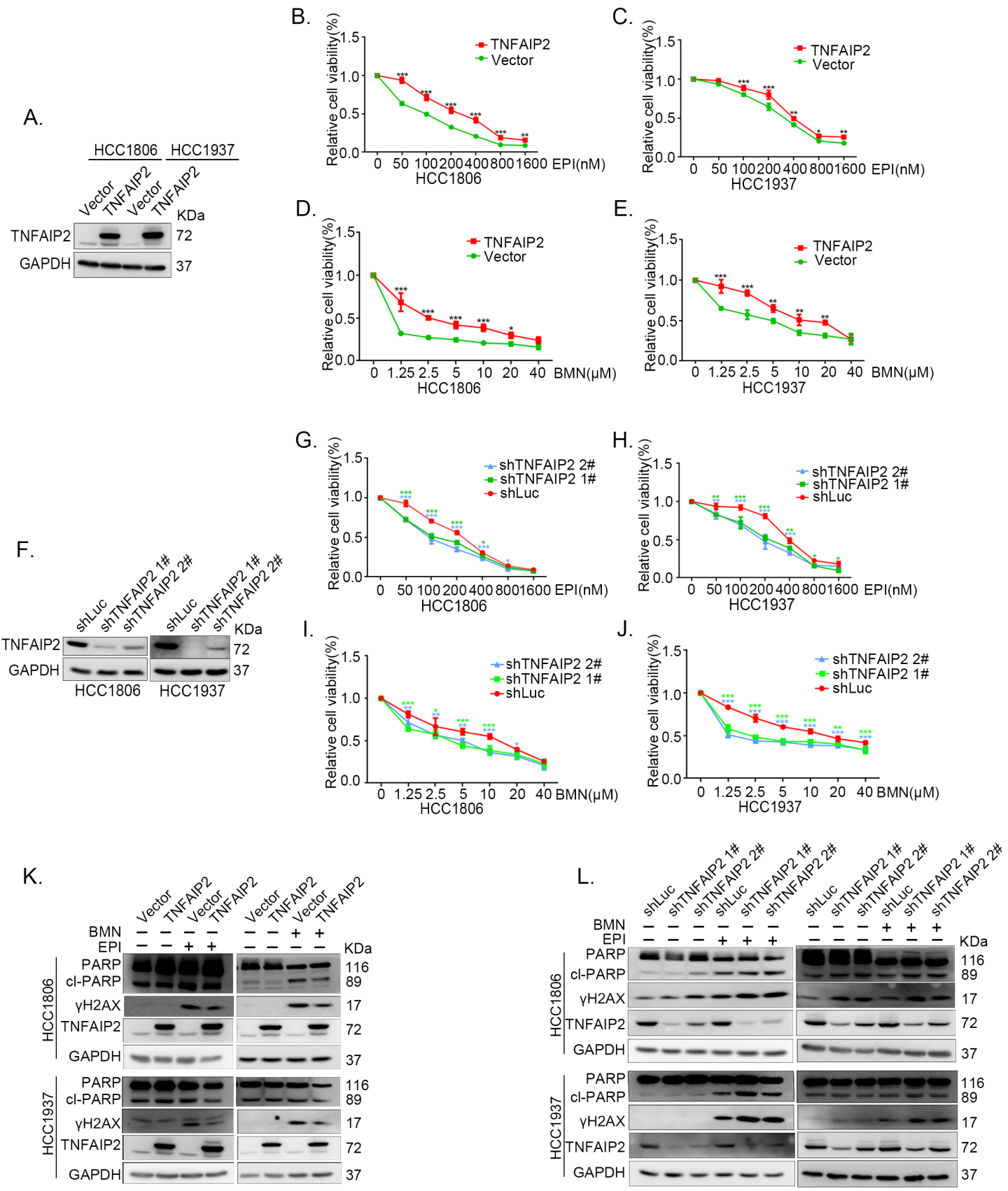
A.
HCC1806
HCC1937
Vector
TNFAIP2
Vector
TNFAIP2
KDa
TNFAIP2
GAPDH
72
37
B.
C.
D.
E.
Relative cell viability(%)
TNFAIP2
Vector
0 50 100 200 400 800 1600 EPI(nM)
0 1.25 2.5 5 10 20 40 BMN(μM)
HCC1806
HCC1937
F.
shLuc
shTNFAIP2 1#
shTNFAIP2 2#
G.
H.
I.
J.
K.
L.
BMN
EPI
PARP
cl-PARP
γH2AX
116
89
17
K.
L.

Figure 1

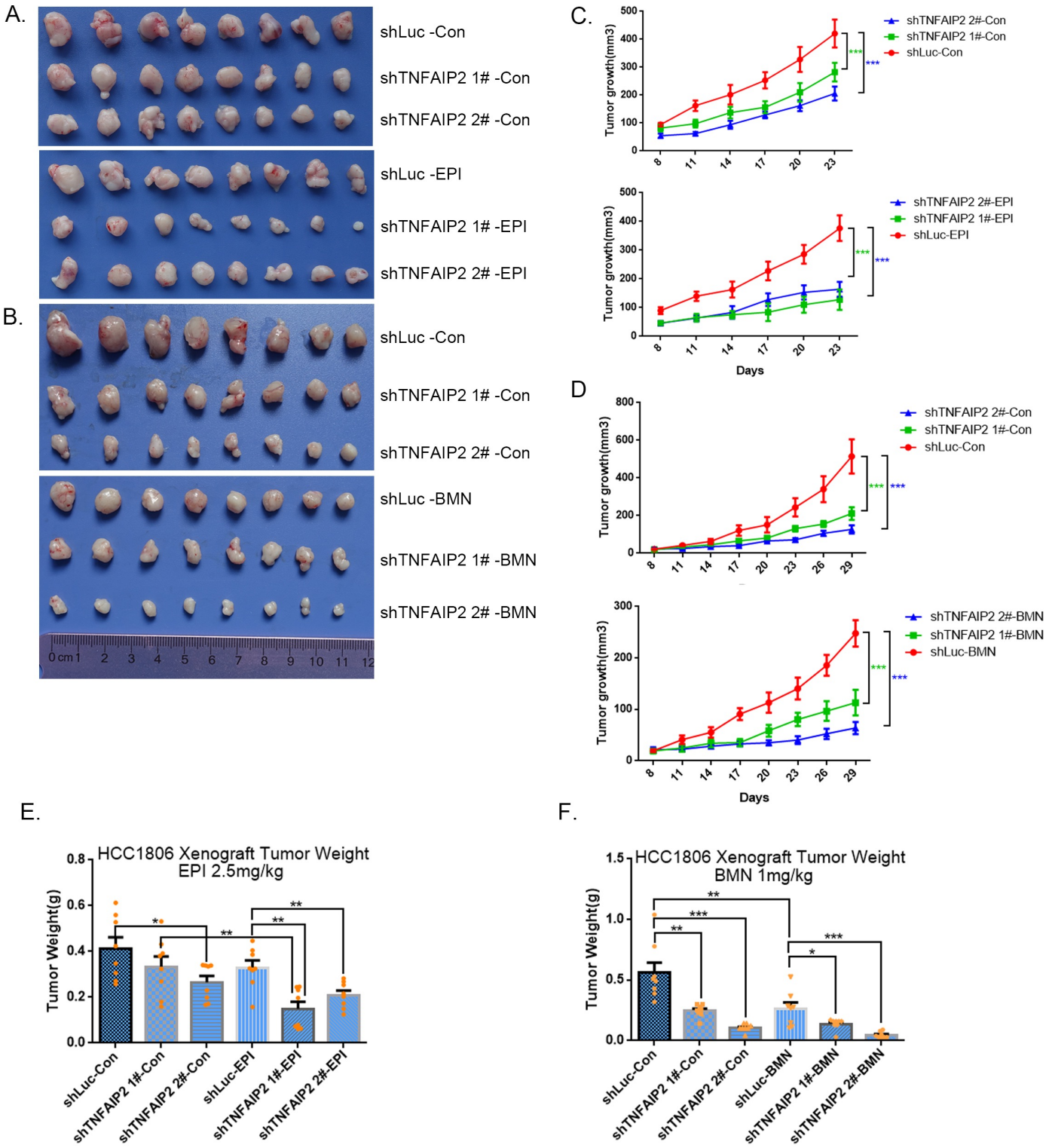
A.
shLuc -Con
shTNFAIP2 1# -Con
shTNFAIP2 2# -Con
shLuc -EPI
shTNFAIP2 1# -EPI
shTNFAIP2 2# -EPI
B.
shLuc -Con
shTNFAIP2 1# -Con
shTNFAIP2 2# -Con
shLuc -BMN
shTNFAIP2 1# -BMN
shTNFAIP2 2# -BMN
0 cm 1 2 3 4 5 6 7 8 9 10 11 12
C.
Tumor growth(mm3)
shTNFAIP2 2#-Con
shTNFAIP2 1#-Con
shLuc-Con
shTNFAIP2 2#-EPI
shTNFAIP2 1#-EPI
shLuc-EPI
Days
D
shTNFAIP2 2#-BMN
shTNFAIP2 1#-BMN
shLuc-BMN
E.
HCC1806 Xenograft Tumor Weight
EPI 2.5mg/kg
Tumor Weight(g)
shLuc-Con
shTNFAIP2 1#-Con
shTNFAIP2 2#-Con
shLuc-EPI
shTNFAIP2 1#-EPI
shTNFAIP2 2#-EPI
F.
HCC1806 Xenograft Tumor Weight
BMN 1mg/kg
shLuc-BMN
shTNFAIP2 1#-BMN
shTNFAIP2 2#-BMN

Figure 2

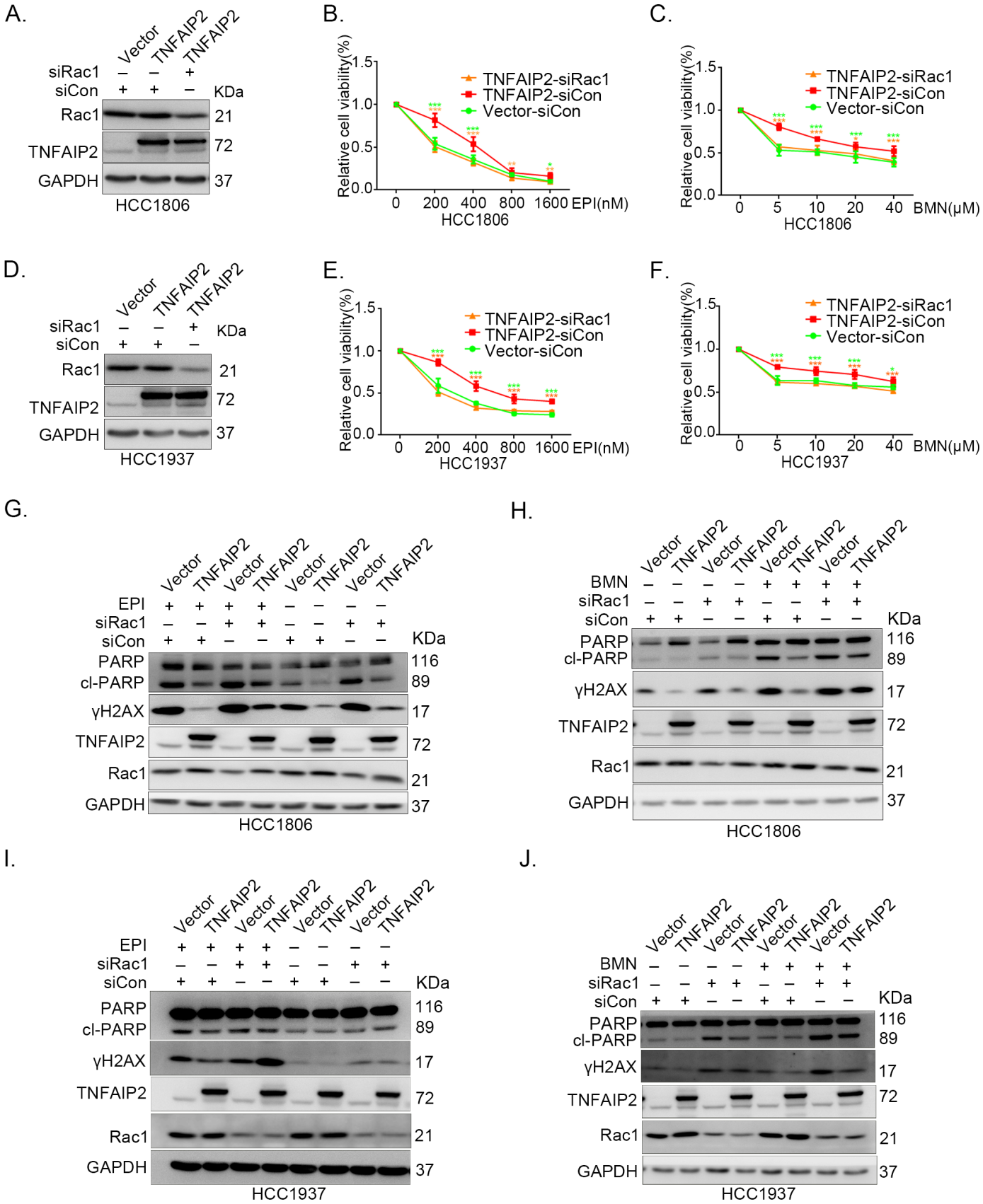
A.
Vector
TNFAIP2
TNFAIP2
siRac1 – – +
siCon + + –
KDa
Rac1 21
TNFAIP2 72
GAPDH 37
HCC1806
B.
Relative cell viability(%)
TNFAIP2-siRac1
TNFAIP2-siCon
Vector-siCon
0 200 400 800 1600 EPI(nM)
HCC1806
C.
Relative cell viability(%)
TNFAIP2-siRac1
TNFAIP2-siCon
Vector-siCon
0 5 10 20 40 BMN(μM)
HCC1806
D.
Vector
TNFAIP2
TNFAIP2
siRac1 – – +
siCon + + –
KDa
Rac1 21
TNFAIP2 72
GAPDH 37
HCC1937
E.
Relative cell viability(%)
TNFAIP2-siRac1
TNFAIP2-siCon
Vector-siCon
0 200 400 800 1600 EPI(nM)
HCC1937
F.
Relative cell viability(%)
TNFAIP2-siRac1
TNFAIP2-siCon
Vector-siCon
0 5 10 20 40 BMN(μM)
HCC1937
G.
Vector TNFAIP2 Vector TNFAIP2 Vector TNFAIP2 Vector TNFAIP2
EPI + + + + – – – –
siRac1 – – + + – – + +
siCon + + – – + + – –
KDa
PARP 116
cl-PARP 89
γH2AX 17
TNFAIP2 72
Rac1 21
GAPDH 37
HCC1806
H.
Vector TNFAIP2 Vector TNFAIP2 Vector TNFAIP2 Vector TNFAIP2
BMN – – – – + + + +
siRac1 – – + + – – + +
siCon + + – – + + – –
KDa
PARP 116
cl-PARP 89
γH2AX 17
TNFAIP2 72
Rac1 21
GAPDH 37
HCC1806
I.
Vector TNFAIP2 Vector TNFAIP2 Vector TNFAIP2 Vector TNFAIP2
EPI + + + + – – – –
siRac1 – – + + – – + +
siCon + + – – + + – –
KDa
PARP 116
cl-PARP 89
γH2AX 17
TNFAIP2 72
Rac1 21
GAPDH 37
HCC1937
J.
Vector TNFAIP2 Vector TNFAIP2 Vector TNFAIP2 Vector TNFAIP2
BMN – – – – + + + +
siRac1 – – + + – – + +
siCon + + – – + + – –
KDa
PARP 116
cl-PARP 89
γH2AX 17
TNFAIP2 72
Rac1 21
GAPDH 37
HCC1937

Figure 3

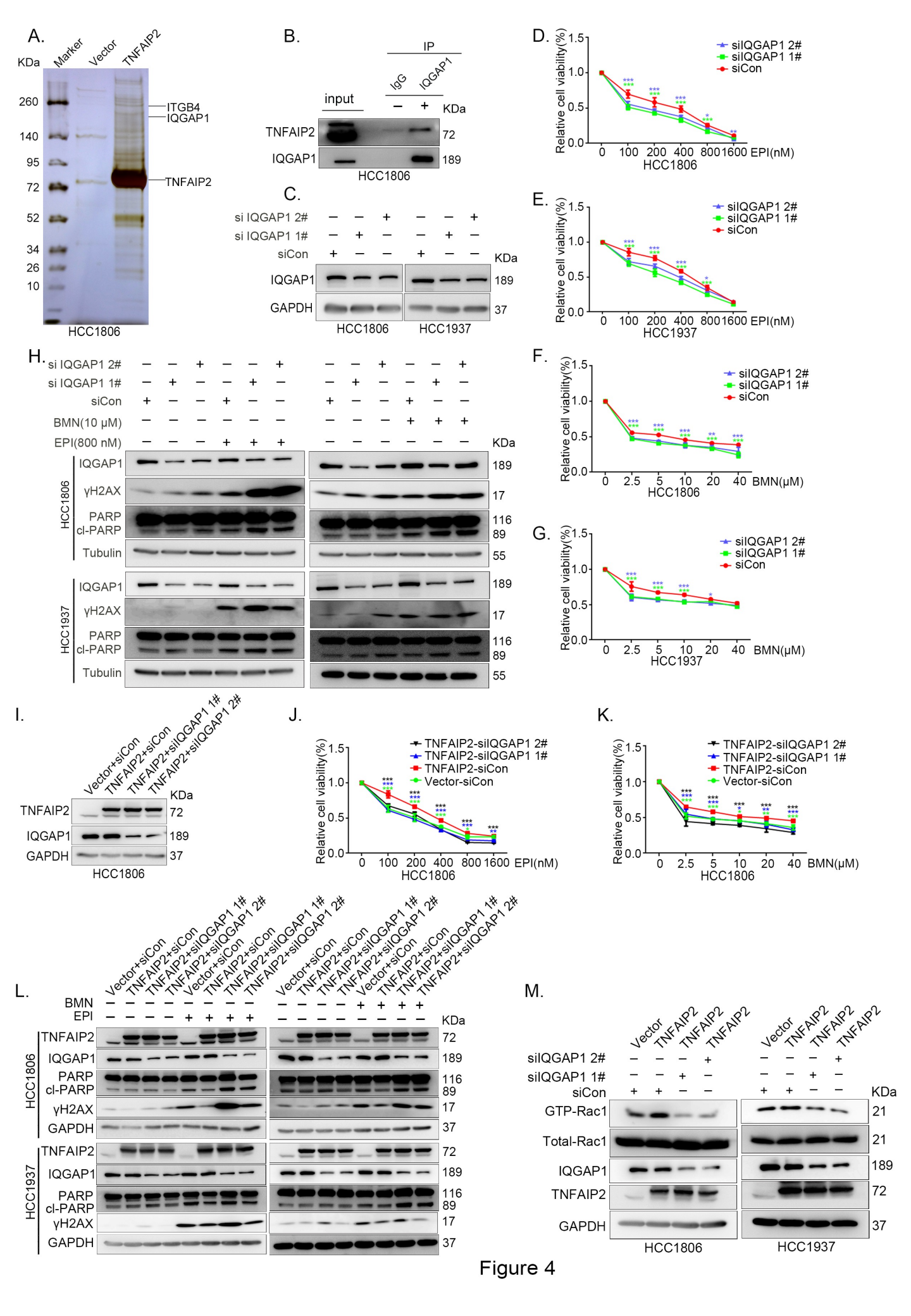
A.
Marker
Vector
TNFAIP2
KDa
260
140
95
72
52
34
26
10
ITGB4
IQGAP1
TNFAIP2
HCC1806
B.
IP
IgG
IQGAP1
input
KDa
TNFAIP2
IQGAP1
72
189
HCC1806
C.
si IQGAP1 2#
si IQGAP1 1#
siCon
KDa
IQGAP1
GAPDH
189
37
HCC1806
HCC1937
D.
siIQGAP1 2#
siIQGAP1 1#
siCon
Relative cell viability(%)
EPI(nM)
HCC1806
E.
siIQGAP1 2#
siIQGAP1 1#
siCon
Relative cell viability(%)
EPI(nM)
HCC1937
F.
siIQGAP1 2#
siIQGAP1 1#
siCon
Relative cell viability(%)
BMN(μM)
HCC1806
G.
siIQGAP1 2#
siIQGAP1 1#
siCon
Relative cell viability(%)
BMN(μM)
HCC1937
H.
si IQGAP1 2#
si IQGAP1 1#
siCon
BMN(10 μM)
EPI(800 nM)
KDa
HCC1806
HCC1937
IQGAP1
γH2AX
PARP
cl-PARP
Tubulin
189
17
116
89
55
I.
Vector+siCon
TNFAIP2+siCon
TNFAIP2+siIQGAP1 1#
TNFAIP2+siIQGAP1 2#
KDa
TNFAIP2
IQGAP1
GAPDH
72
189
37
HCC1806
J.
TNFAIP2-siIQGAP1 2#
TNFAIP2-siIQGAP1 1#
TNFAIP2-siCon
Vector-siCon
Relative cell viability(%)
EPI(nM)
HCC1806
K.
TNFAIP2-siIQGAP1 2#
TNFAIP2-siIQGAP1 1#
TNFAIP2-siCon
Vector-siCon
Relative cell viability(%)
BMN(μM)
HCC1806
L.
Vector+siCon
TNFAIP2+siCon
TNFAIP2+siIQGAP1 1#
TNFAIP2+siIQGAP1 2#
BMN
EPI
KDa
HCC1806
HCC1937
TNFAIP2
IQGAP1
PARP
cl-PARP
γH2AX
GAPDH
72
189
116
89
17
37
M.
Vector
TNFAIP2
siIQGAP1 2#
siIQGAP1 1#
siCon
KDa
GTP-Rac1
Total-Rac1
IQGAP1
TNFAIP2
GAPDH
21
189
72
37
HCC1806
HCC1937

Figure 4

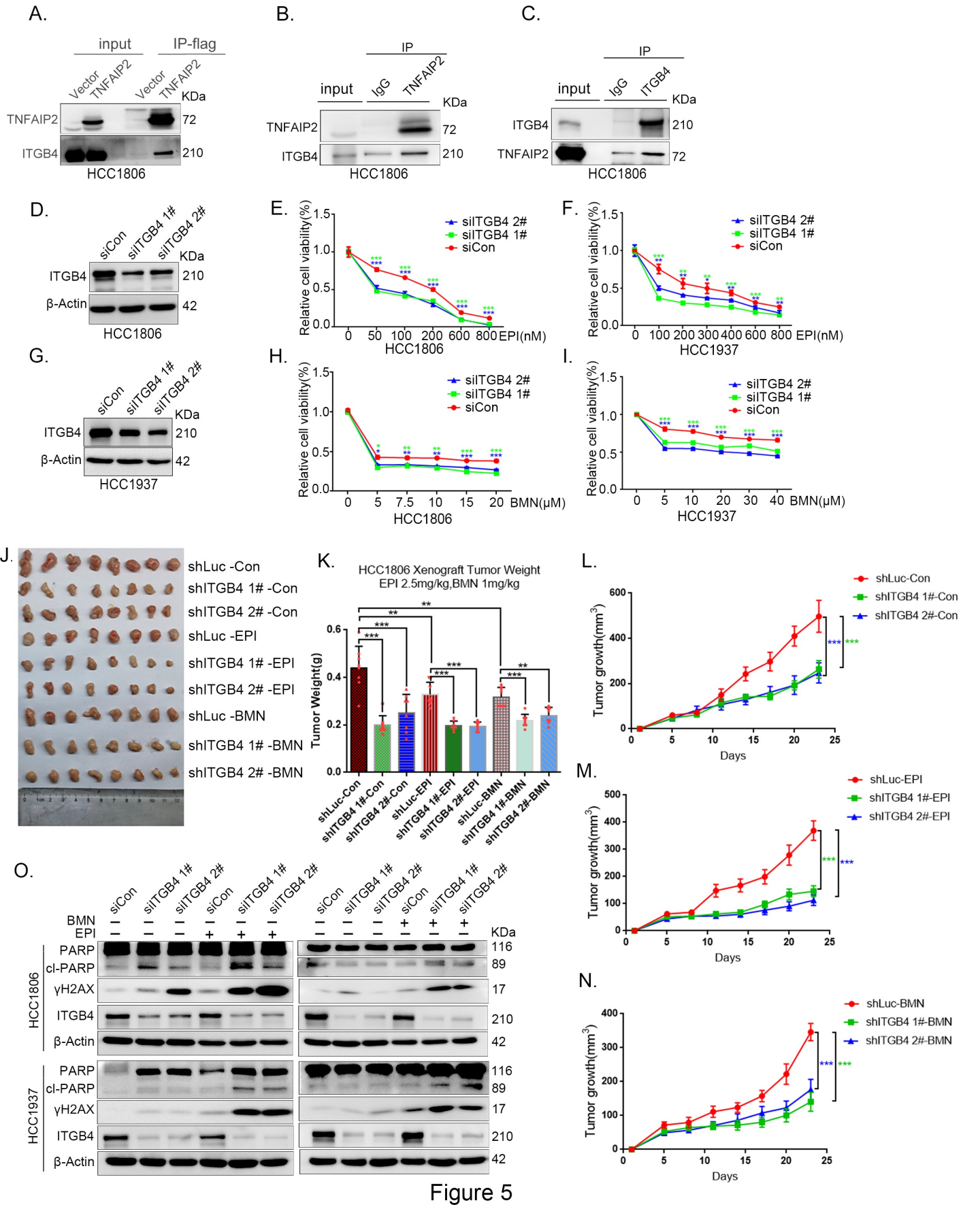
A.
input
IP-flag
Vector
TNFAIP2
Vector
TNFAIP2
KDa
TNFAIP2
72
ITGB4
210
HCC1806
B.
IP
input
IgG
TNFAIP2
KDa
TNFAIP2
72
ITGB4
210
HCC1806
C.
IP
input
IgG
ITGB4
KDa
ITGB4
210
TNFAIP2
72
HCC1806
D.
siCon
siITGB4 1#
siITGB4 2#
KDa
ITGB4
210
β-Actin
42
HCC1806
E.
Relative cell viability(%)
siITGB4 2#
siITGB4 1#
siCon
EPI(nM)
HCC1806
F.
Relative cell viability(%)
siITGB4 2#
siITGB4 1#
siCon
EPI(nM)
HCC1937
G.
siCon
siITGB4 1#
siITGB4 2#
KDa
ITGB4
210
β-Actin
42
HCC1937
H.
Relative cell viability(%)
siITGB4 2#
siITGB4 1#
siCon
BMN(μM)
HCC1806
I.
Relative cell viability(%)
siITGB4 2#
siITGB4 1#
siCon
BMN(μM)
HCC1937
J.
shLuc -Con
shITGB4 1# -Con
shITGB4 2# -Con
shLuc -EPI
shITGB4 1# -EPI
shITGB4 2# -EPI
shLuc -BMN
shITGB4 1# -BMN
shITGB4 2# -BMN
K.
HCC1806 Xenograft Tumor Weight
EPI 2.5mg/kg,BMN 1mg/kg
Tumor Weight(g)
shLuc-Con
shITGB4 1#-Con
shITGB4 2#-Con
shLuc-EPI
shITGB4 1#-EPI
shITGB4 2#-EPI
shLuc-BMN
shITGB4 1#-BMN
shITGB4 2#-BMN
L.
Tumor growth(mm3)
Days
shLuc-Con
shITGB4 1#-Con
shITGB4 2#-Con
M.
Tumor growth(mm3)
Days
shLuc-EPI
shITGB4 1#-EPI
shITGB4 2#-EPI
N.
Tumor growth(mm3)
Days
shLuc-BMN
shITGB4 1#-BMN
shITGB4 2#-BMN
O.
siCon
siITGB4 1#
siITGB4 2#
BMN
EPI
KDa
HCC1806
HCC1937
PARP
cl-PARP
γH2AX
ITGB4
β-Actin
116
89
17
210
42

Figure 5

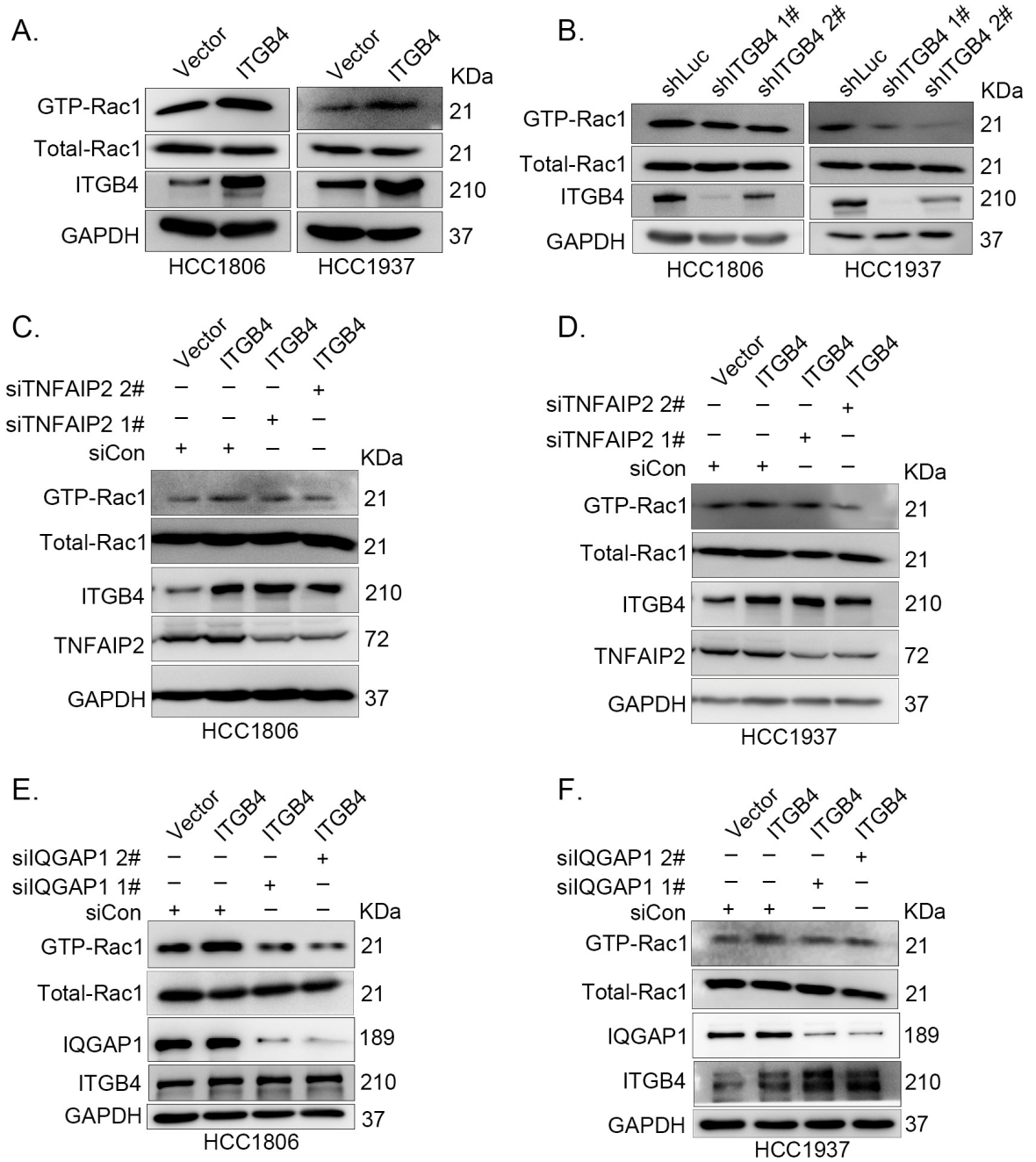
A.
Vector
ITGB4
Vector
ITGB4
KDa
GTP-Rac1
Total-Rac1
ITGB4
GAPDH
21
21
210
37
HCC1806
HCC1937
B.
shLuc
shITGB4 1#
shITGB4 2#
shLuc
shITGB4 1#
shITGB4 2#
KDa
GTP-Rac1
Total-Rac1
ITGB4
GAPDH
21
21
210
37
HCC1806
HCC1937
C.
Vector
ITGB4
ITGB4
ITGB4
siTNFAIP2 2#
siTNFAIP2 1#
siCon
KDa
GTP-Rac1
Total-Rac1
ITGB4
TNFAIP2
GAPDH
21
21
210
72
37
HCC1806
D.
Vector
ITGB4
ITGB4
ITGB4
siTNFAIP2 2#
siTNFAIP2 1#
siCon
KDa
GTP-Rac1
Total-Rac1
ITGB4
TNFAIP2
GAPDH
21
21
210
72
37
HCC1937
E.
Vector
ITGB4
ITGB4
ITGB4
siIQGAP1 2#
siIQGAP1 1#
siCon
KDa
GTP-Rac1
Total-Rac1
IQGAP1
ITGB4
GAPDH
21
21
189
210
37
HCC1806
F.
Vector
ITGB4
ITGB4
ITGB4
siIQGAP1 2#
siIQGAP1 1#
siCon
KDa
GTP-Rac1
Total-Rac1
IQGAP1
ITGB4
GAPDH
21
21
189
210
37
HCC1937

Figure 6

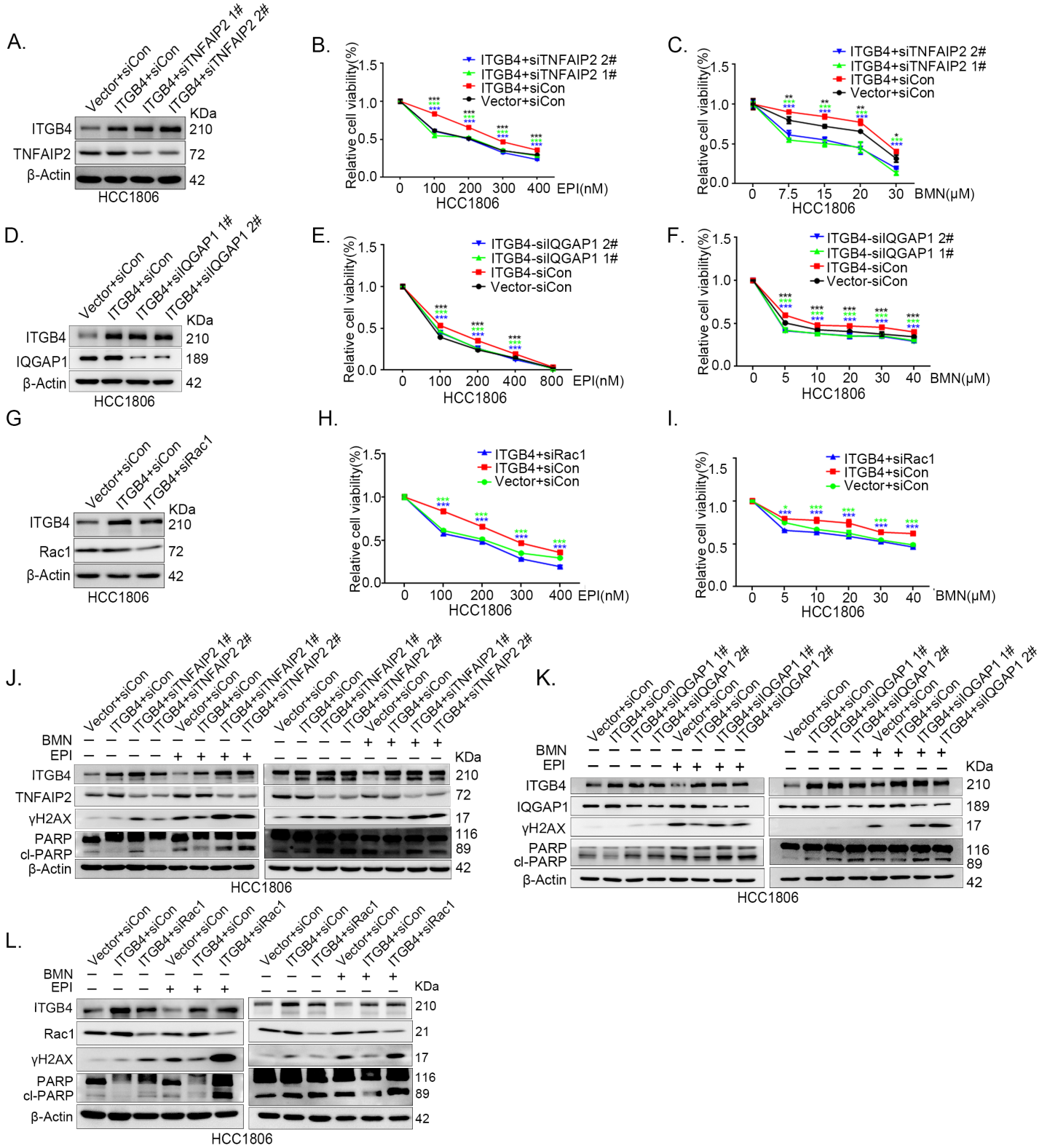
A.
Vector+siCon
ITGB4+siCon
ITGB4+siTNFAIP2 1#
ITGB4+siTNFAIP2 2#
KDa
ITGB4 210
TNFAIP2 72
β-Actin 42
HCC1806
B.
ITGB4+siTNFAIP2 2#
ITGB4+siTNFAIP2 1#
ITGB4+siCon
Vector+siCon
Relative cell viability(%)
EPI(nM)
HCC1806
C.
ITGB4+siTNFAIP2 2#
ITGB4+siTNFAIP2 1#
ITGB4+siCon
Vector+siCon
Relative cell viability(%)
BMN(μM)
HCC1806
D.
Vector+siCon
ITGB4+siCon
ITGB4+siIQGAP1 1#
ITGB4+siIQGAP1 2#
KDa
ITGB4 210
IQGAP1 189
β-Actin 42
HCC1806
E.
ITGB4-siIQGAP1 2#
ITGB4-siIQGAP1 1#
ITGB4-siCon
Vector-siCon
Relative cell viability(%)
EPI(nM)
HCC1806
F.
ITGB4-siIQGAP1 2#
ITGB4-siIQGAP1 1#
ITGB4-siCon
Vector-siCon
Relative cell viability(%)
BMN(μM)
HCC1806
G
Vector+siCon
ITGB4+siCon
ITGB4+siRac1
KDa
ITGB4 210
Rac1 72
β-Actin 42
HCC1806
H.
ITGB4+siRac1
ITGB4+siCon
Vector+siCon
Relative cell viability(%)
EPI(nM)
HCC1806
I.
ITGB4+siRac1
ITGB4+siCon
Vector+siCon
Relative cell viability(%)
BMN(μM)
HCC1806
J.
Vector+siCon
ITGB4+siCon
ITGB4+siTNFAIP2 1#
ITGB4+siTNFAIP2 2#
BMN
EPI
KDa
ITGB4 210
TNFAIP2 72
γH2AX 17
PARP 116
cl-PARP 89
β-Actin 42
HCC1806
K.
Vector+siCon
ITGB4+siCon
ITGB4+siIQGAP1 1#
ITGB4+siIQGAP1 2#
BMN
EPI
KDa
ITGB4 210
IQGAP1 189
γH2AX 17
PARP 116
cl-PARP 89
β-Actin 42
HCC1806
L.
Vector+siCon
ITGB4+siCon
ITGB4+siRac1
BMN
EPI
KDa
ITGB4 210
Rac1 21
γH2AX 17
PARP 116
cl-PARP 89
β-Actin 42
HCC1806

Figure 7

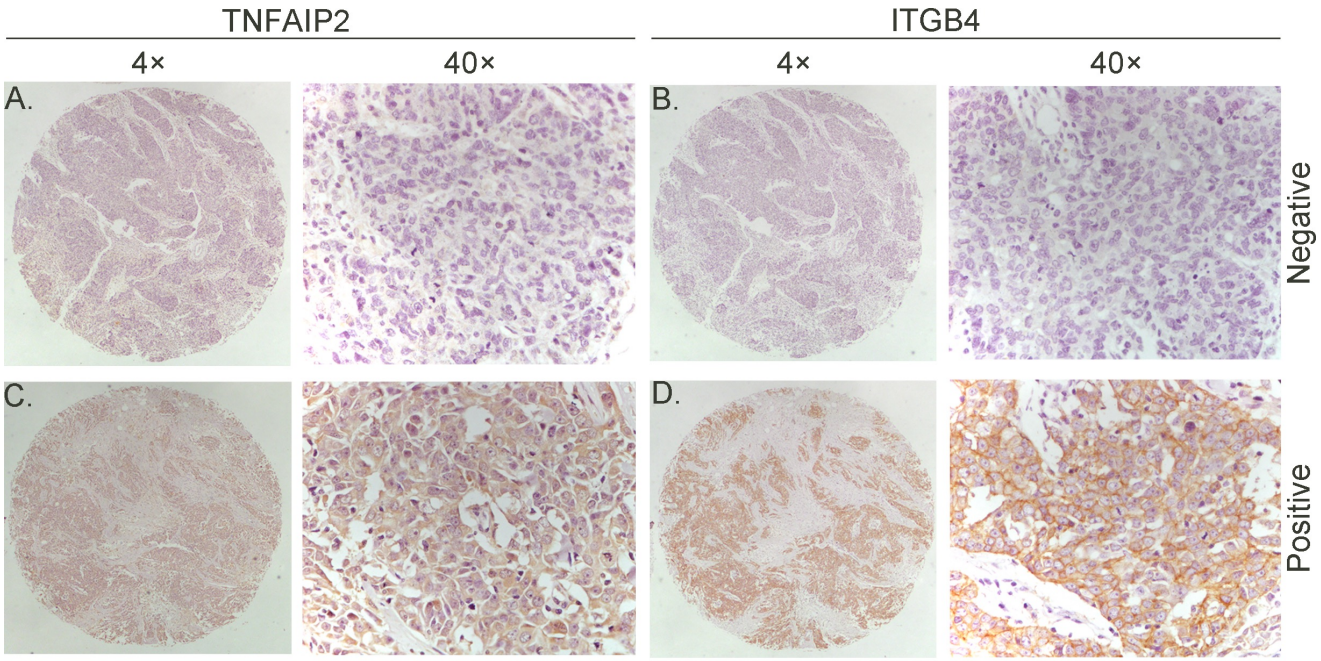

E.

R=0.528 P<0.01		TNFAIP2		
		Negative	Positive	Total
ITGB4	Negative	51	16	67
	Positive	26	42	68
	Total	77	58	135

F.

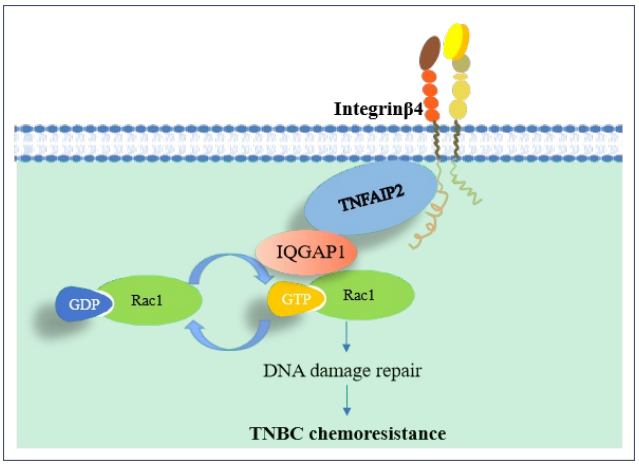

Figure 8